RESEARCH ARTICLE

VOLCANICA

Temporal and morphological eruption characteristics of lava flows from the Holocene La Taza monogenetic cone obtained from petrology and LiDAR imagery (Michoacán, Mexico)

Geoffrey A. Lerner* [α,β], Claus Siebe[α], Israel Ramírez-Uribe[α], and Christopher T. Fisher[γ]

[α] Departamento de Vulcanología, Instituto de Geofísica, Universidad Nacional Autónoma de México, Coyoacán, C.P. 04510, Ciudad de México, Mexico.

[β] Earth Observatory of Singapore, Nanyang Technological University, Singapore.

[γ] Department of Anthropology, Colorado State University, Fort Collins, CO-80523, USA.

Abstract

The Holocene La Taza andesitic volcano is one of over 1000 volcanic centers located within the Michoacán-Guanajuato Volcanic Field (MGVF) in central-western Mexico. La Taza (~8500–8200 yr BP) represents one possible eruption style within the field, with deposits indicating Strombolian activity followed by a series of lava flows. In our study, we reconstruct the eruption of La Taza through a combination of LiDAR mapping and petrological and geochemical analyses. LiDAR mapping combined with ground-truthing in the field allowed us to differentiate and determine the sequence of the volcano's lava flows, revealing seven lava flows with a volume of ~0.6 km^3. This morphological information was paired with geothermobarometers to estimate lava flow viscosities, mean effusion rates, and emplacement times, showing a likely duration of 1.1–4.3 years. Recreating this eruption contributes to the understanding of potential durations and lava flow rheology of future MGVF eruptions, crucial characteristics for hazard planning and mitigation.

Resumen

El volcán andesítico La Taza del Holoceno es uno de los más de 1000 centros volcánicos ubicados dentro del Campo Volcánico Michoacán-Guanajuato (MGVF) en el centro-oeste de México. La Taza (~8,500–8,200 años AP) representa un posible estilo de erupción dentro del campo, con depósitos que indican actividad estromboliana seguida de una serie de flujos de lava. En nuestro estudio, reconstruimos la erupción de La Taza mediante una combinación de mapeo LiDAR y análisis petrográficos y geoquímicos. El mapeo LiDAR, combinado con el trabajo de campo, nos permitió diferenciar y determinar la secuencia de los flujos de lava del volcán, revelando siete flujos de lava con un volumen de ~0.6 km^3. Esta información morfológica en conjunto con geotermobarómetros permitió estimar viscosidades de los flujos de lava, tasas de efusión media y tiempos de emplazamiento, mostrando una probable duración de 1.1 a 4.3 años. La reconstrucción de esta erupción contribuye a la comprensión de las posibles duraciones y la reología de los flujos de lava en futuras erupciones del Campo Volcánico Michoacán-Guanajuato, características cruciales para la planificación y mitigación de riesgos.

Keywords: Volcanic field; Monogenetic volcanism; Mexico; Michoacan; Viscosity; Lava flow.

Submitted: 2023-11-24 | Accepted: 2024-06-21 | Published: 2024-09-04

Editor: A Whittington | Typesetter: J Farquharson

1 Introduction

Distributed volcanic fields are characterized by varying types of volcanic structures that are emplaced across large geographic areas over long periods of time [Valentine and Connor 2015]. The long repose times, varying sizes and styles of eruptions, and uncertainties about future vent locations create significant difficulty for hazard planning and mitigation in volcanic fields [Hayes et al. 2020].

Given that common styles of eruption within volcanic fields typically involve significant effusive activity (e.g. scoria cones and shields), lava flows are one of the primary volcanic hazards present in distributed volcanic fields [Valentine and Connor 2015]. This hazard is heavily dependent on lava rheology, effusion rate, and eruption duration [Harris 2015; Kilburn 2015]. These characteristics affect: 1) the probability that lava from a vent located near a populated area will reach a distance necessary to impact people and infrastructure, 2) how long people will have to plan or evacuate once the vent location is known, and 3) how long affected populations will have to live with the hazard from the ongoing eruption [Harris 2015; Tsang and Lindsay 2020].

Lava flows from previous eruptions can be vital tools for understanding these characteristics in order to better evaluate lava flow dynamics and hazards in future eruptions. Evolution of active lava flows is dependent on effusion rate, underlying topography, and lava rheology (which changes during the eruption and cooling of the flows) [e.g. Castruccio et al. 2013; Tsang and Lindsay 2020]. Direct measurements of viscosities of evolved andesitic lava are difficult to make, so few field or lab measurements exist, especially prior to recent years [Chevrel et al. 2015; 2019]. Therefore, post-eruption evaluation of the structure of lava flows has often been useful for understanding flow rheology [Hulme 1974; Griffiths 2000].

More recently, numerical lava flow models can be used to assess lava flow hazard based on morphological and petrological characteristics, while rheological models can determine lava viscosity from their morphological characteristics [e.g. Connor et al. 2012; Lev et al. 2012; Cappello et al. 2016b].

* geoffrey.lerner@ntu.edu.sg

Studies based on analysis of lava deposits from past eruptions provide empirical evidence useful for better calibrating these models [Lev et al. 2012; Kubanek et al. 2015; Pistone et al. 2016]. Models which assess hazard and risk related to lava flows can benefit from more refined inputs related to characteristics like duration and rheology [e.g. Cappello et al. 2016a; Tsang et al. 2019; Verolino et al. 2022].

Like many distributed volcanic fields, the Michoacán-Guanajuato Volcanic Field (MGVF) in central Mexico has shown a wide variety of eruption styles, sizes, and durations [Hasenaka and Carmichael 1985; Guilbaud et al. 2012; Kshirsagar et al. 2016]. The MGVF is located along an active subduction zone and has a long history of volcanism, including two historic eruptions from Jorullo (1759–1774) and Paricutin (1943–1952) scoria cones [Luhr and Simkin 1993; Guilbaud et al. 2011; Larrea et al. 2017]. Lava flows during these eruptions caused the destruction of agricultural land (in the case of Jorullo) and buried two small towns, requiring permanent relocation of their entire population (in the case of Paricutin); both eruptions had significant economic and social impacts [Luhr and Simkin 1993; Guilbaud et al. 2009]. This history, combined with recurrent recent seismic swarms [Legrand et al. 2023], suggests a likely eruption at some point in the future. However, uncertainty about future vent locations, as well as the style and duration of future eruptions, makes hazard planning and mitigation in such a large region difficult.

More recently, a number of studies have addressed eruption types and lava rheology within the MGVF, providing detailed studies of individual volcanic structures and groups within the field [e.g. Guilbaud et al. 2011; 2012; Chevrel et al. 2016a; Larrea et al. 2017; 2019a; b; Ramírez-Uribe et al. 2021; Reyes-Guzmán et al. 2021]. These studies represent the start of a catalogue of eruption types represented by past activity in the MGVF, especially effusive events, which provides useful information about potential future eruption styles.

Here we contribute to the understanding of potential future eruption scenarios in the MGVF through a case study of a mostly effusive Holocene scoria cone eruption at La Taza monogenetic cone. By using high-resolution LiDAR data along with petrographic and geochemical methods, we recreate the eruption chronology of the La Taza eruption and calculate a number of key eruptive characteristics, including the viscosities and velocities of the lava flows and the mean output rate and duration of the eruption.

2 Geological Setting

2.1 Michoacán-Guanajuato Volcanic Field (MGVF)

The MGVF is a distributed volcanic field consisting of over 1400 Quaternary monogenetic eruptive centers across an area of ~40,000 km^2 [Hasenaka and Carmichael 1985] (Figure 1). It is located in the central part of the Trans-Mexican Volcanic Belt (TMVB), which includes ~3,000 visible monogenetic structures from the west to east coast of central Mexico [Siebe et al. 2014]. The TMVB results from the subduction of the Cocos and Rivera oceanic plates beneath the North American continental plate along the Mesoamerican trench [Nixon 1982; Pardo and Suárez 1995; Gómez-Tuena et al. 2005]. Geographically, the MGVF is bounded to the north by the Lerma River valley, to the south by the Balsas River depression, to the west by the Mazamitla Volcanic Gap, and to the east by the Tzitzio anticline [Blatter and Hammersley 2010; Kshirsagar et al. 2015] (Figure 1).

The MGVF is generally considered the highest concentration of subduction zone monogenetic volcanism in the world [Hasenaka and Carmichael 1985; Hasenaka 1994]. During its activity spanning the Pleistocene and Holocene, the MGVF has produced primarily monogenetic volcanoes displaying a wide variety in size, style, duration, and frequency of eruptions [e.g. Guilbaud et al. 2011; 2012; Siebe et al. 2014; Kshirsagar et al. 2015; Chevrel et al. 2016a; Kshirsagar et al. 2016; Larrea et al. 2017; Osorio-Ocampo et al. 2018; Pérez-Orozco et al. 2018; Guilbaud et al. 2019; Larrea et al. 2019a; Ramírez-Uribe et al. 2019; Reyes-Guzmán et al. 2021] (Figure 2). Structures and deposits within the MGVF are generally calc-alkaline in composition [Hasenaka and Carmichael 1987; Gómez-Tuena et al. 2005]. The most common features are scoria cones and their associated lava flows, but the field also contains isolated thick lava flows and domes, maars, tuff rings, and ~400 small to medium-size shield volcanoes [Hasenaka and Carmichael 1985; Hasenaka 1994; Chevrel et al. 2016a]. There are also two extinct stratovolcanoes, Tancítaro and Patamban [Ownby et al. 2007; Siebe et al. 2014].

2.2 La Taza

La Taza volcano is an andesitic monogenetic scoria cone located 7 km from the shore of Pátzcuaro Lake and 12 km from the nearest large population center, the city of Pátzcuaro [Osorio-Ocampo et al. 2018] (Figure 2). The scoria cone has an elevation of 2345 m and is situated on the W margin of the Pátzcuaro lake basin (Figure 3A,3B), ~190 m above the lake. The volcano has a lava flow field extending towards the lake to its north, representing a series of lava flows which overlie a thin tephra sequence [Osorio-Ocampo et al. 2018, Figure 3B, 3C]. The volcano and its flow field cover an area of 15 km^2 (Figure 4). Previous radiocarbon dates assign the volcano a maximum age of 8640–8360 cal. yr BCE [Osorio-Ocampo et al. 2018], and a radiocarbon date from this study taken under the paleosol below La Taza tephra confirms a similar maximum age (8710–8290 cal. yr BCE). An older radiocarbon age suggests a potentially younger volcano age (8280–6640 cal. yr BCE [Hasenaka and Carmichael 1985]), while a more recent paleomagnetic study assigns a significantly younger age of 6450 yr BP [García-Quintana et al. 2016]. However, given the relative consistency of the radiocarbon data and the lack of clarity in regard to the exact stratigraphic position of the paleomagnetic sampling site [García-Quintana et al. 2016], we find an age within the range of 8500–8200 cal. yr BCE as the most probable date for the eruption. A table with details of the radiocarbon dates and a photo of the exact position of our paleosol sample obtained directly underneath the La Taza ash fallout are provided in Supplementary Material 1.

The cone and lava flows have not yet been deforested by farmers because the lack of soil development renders the hard substrate unsuitable for agriculture. Hence, most outcrops of

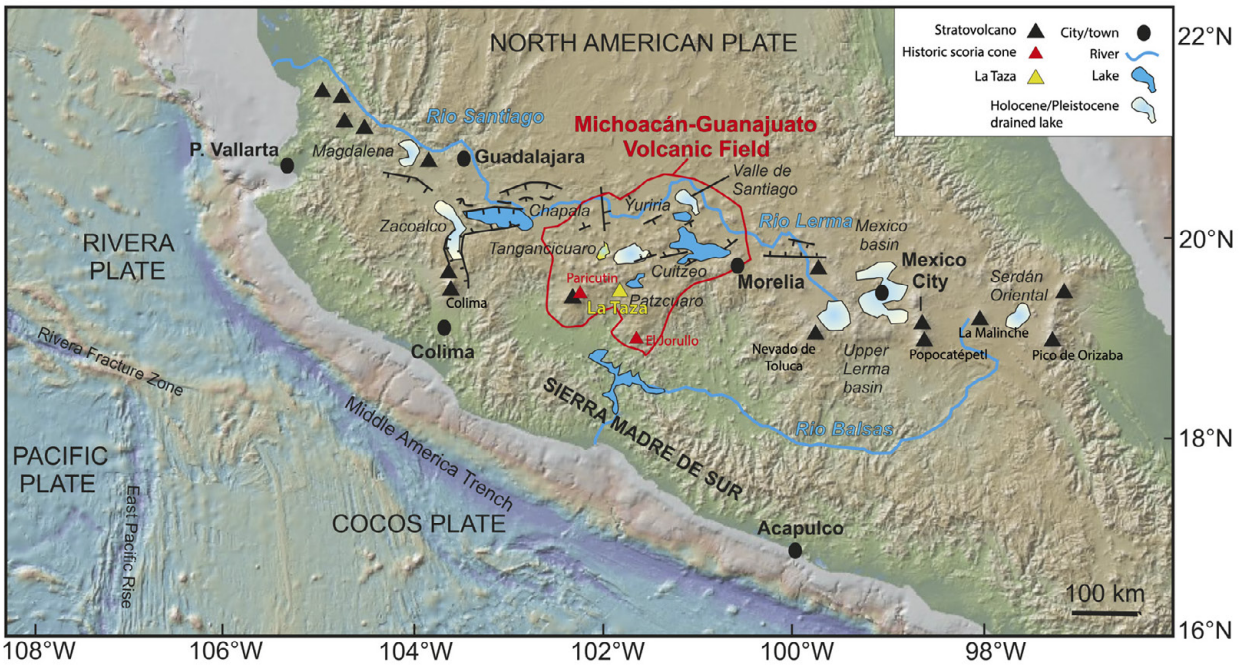

Figure 1: Map of central Mexico showing the tectonic setting of the Trans-Mexican Volcanic Belt. Notable geographic locations, landmarks, and volcanoes are labeled. The Michoacán-Guanajuato Volcanic Field is outlined in red. Modified from [Kshirsagar et al. 2015].

blocky lava flow fronts remain vegetated by oak trees (Figure 3D). The tephra sequence representing an initial Strombolian phase is overlain by the lava flow sequence. The lavas are the uppermost unit in this area except where they have intruded into older lake sediment deposits dated at 32–44 ka (Figure 3E; Israde-Alcántara et al. [2005]).

A large archaeological site of a Tarascan settlement that includes platforms and pyramidal temples, Urichu, is located on the northernmost lava flow of the La Taza flow field [Pollard and Cahue 1999; Pollard et al. 2003] (Figure 4). The Tarascan Empire was a pre-Hispanic civilization existing in western Central Mexico from ~ 1250 CE until the Spanish conquest in 1530 CE [Pollard 2008]. Several pre-Hispanic archaeological sites of urban dimensions have been discovered on Late Pleistocene-Holocene lava flows in Michoacán, and their presence has spurred the acquisition of high-resolution LiDAR (Laser Imaging Detection and Ranging) data [e.g. Fisher and Leisz 2013; Forest 2020; Pereira et al. 2021], which has been also used previously in volcanological studies in this region [e.g. Ramírez-Uribe et al. 2021; Reyes-Guzmán et al. 2021].

3 Methods

3.1 LiDAR lava flow mapping

Airborne laser scanning (ALS), often referred to as airborne LiDAR technology, is a technique used to acquire high-resolution elevation data for selected geographic regions. The technique uses a near infra-red laser fired from an airborne platform, which travels to the ground and returns to provide elevation data [Chase et al. 2012; Harris 2019]. This is typically used to gain a detailed understanding of the topography by creating high-resolution digital terrain models (DTMs), which allows the analyst to digitally remove vegetation to reveal the topography underneath [Chase et al. 2012; Fisher et al. 2017; Harris 2019]. The ability to bypass vegetation allows for the detailed identification of archaeological sites, as well as the definition of morphological characteristics of volcanic structures, in forested areas [Chase et al. 2012; Cashman et al. 2013].

LiDAR data have been used in a number of volcanological studies around the world [Deardorff and Cashman 2012; Cashman et al. 2013; Dietterich and Cashman 2014; Deligne et al. 2016; Dietterich et al. 2018; Hunt et al. 2019; Younger et al. 2019]. More recently, LiDAR data have been used to study Maya [Inomata et al. 2020; McAnany 2020] and Tarascan [Chase et al. 2012; Fisher and Leisz 2013; Fisher et al. 2017; Forest et al. 2018] archaeological sites in Mexico and, consequently, for volcanological studies of some of those sites [Ramírez-Uribe et al. 2021; Reyes-Guzmán et al. 2021; 2023].

At La Taza, a 50-cm-resolution LiDAR DTM acquired for the "Legacies of Resilience: The Lake Pátzcuaro Basin Archaeological Project" (LORE-LPB) [Fisher and Leisz 2013; Fisher et al. 2017] was used to study the Urichu Tarascan archaeological site located on the La Taza lava flows (Figure 4). We have incorporated this dataset into our volcanological study by using it to morphologically differentiate lava flow lobes and interpret the chronological order of the sequence. The high resolution of the DTM allows the observation of detailed flow morphology and relationships between the flows not typically possible with lower resolution digital elevation models

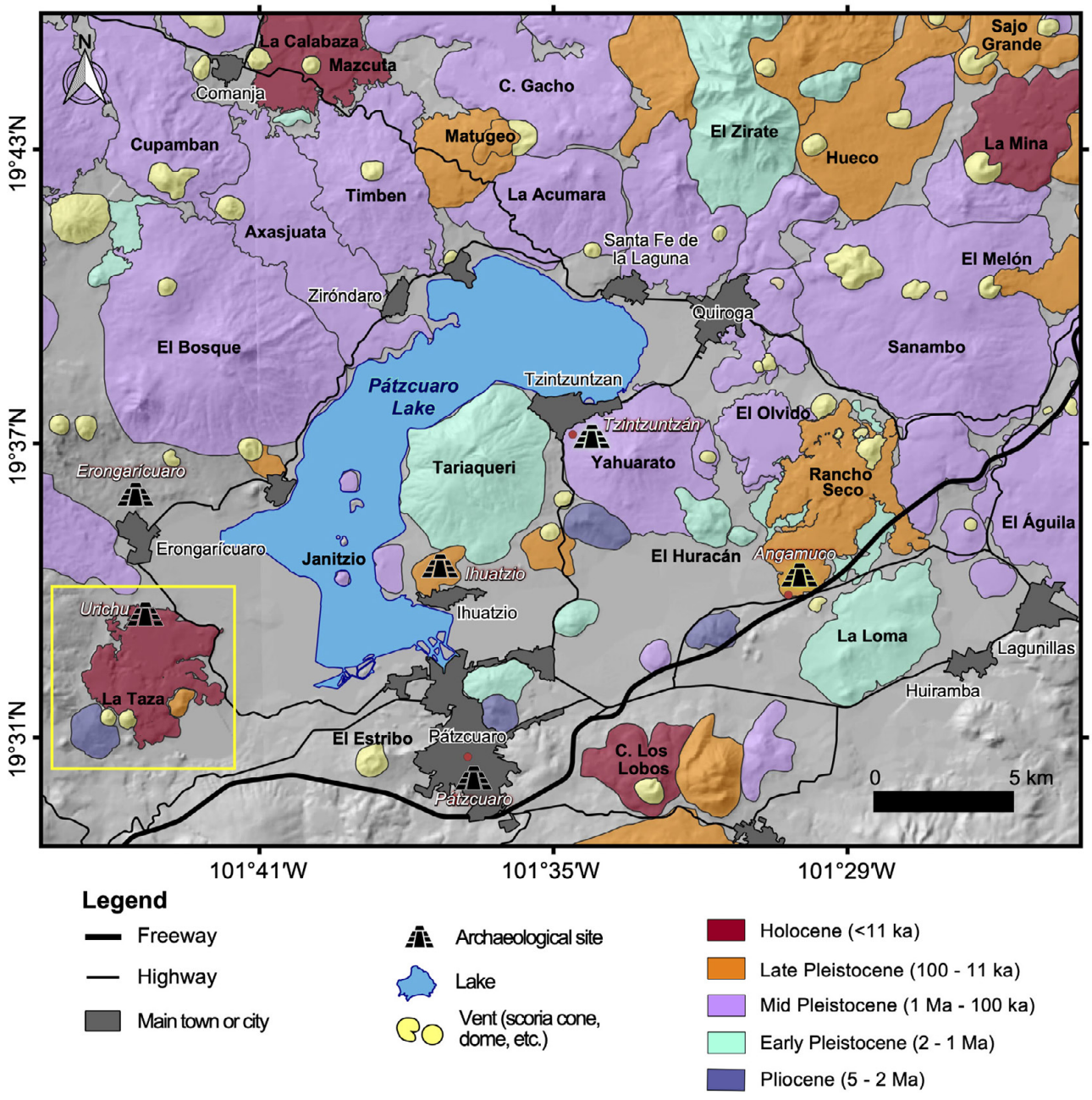

Figure 2: Volcanic geology of the Pátzcuaro Basin located within the Michoacán-Guanajuato Volcanic Field. Archaeological sites built on volcanic deposits are noted. The yellow box highlights the La Taza cone and deposits and the Urichu archaeological site. Modified from [Siebe et al. 2023].

(DEMs), DTMs, or satellite imagery. Field observations were used to ground truth features observed in the LiDAR DTM. Fieldwork involved visiting 18 key locations identified using the DTM to confirm Strombolian deposits, lava flow contacts, cross-cutting relationships, flow fronts, and the limits of the cone and lava field, as well as to collect samples for geochemical analysis, which aided in the interpretation of the eruption chronology. These data and observations were used to create a map detailing the La Taza lava flows and their sequence.

The high-resolution LiDAR also allowed for the calculation of a variety of morphological characteristics of the flows. This included the estimation of volume by comparing the current topography with a modified DEM representing the topography existing prior to the La Taza eruption [Chevrel et al. 2016b] (Figure 5). The "pre-eruption topography" was interpreted by clipping the area representing the cone and flows from the DTM and interpolating the most likely continuation of the 5-m-contour lines for the DTM using the surrounding contours as a guide (Figure 5A,5B). These contours were converted to triangular irregular networks (TIN) using the interpolation plugin in QGIS. This modified topography was then subtracted from the current topography (50 cm DTM) using

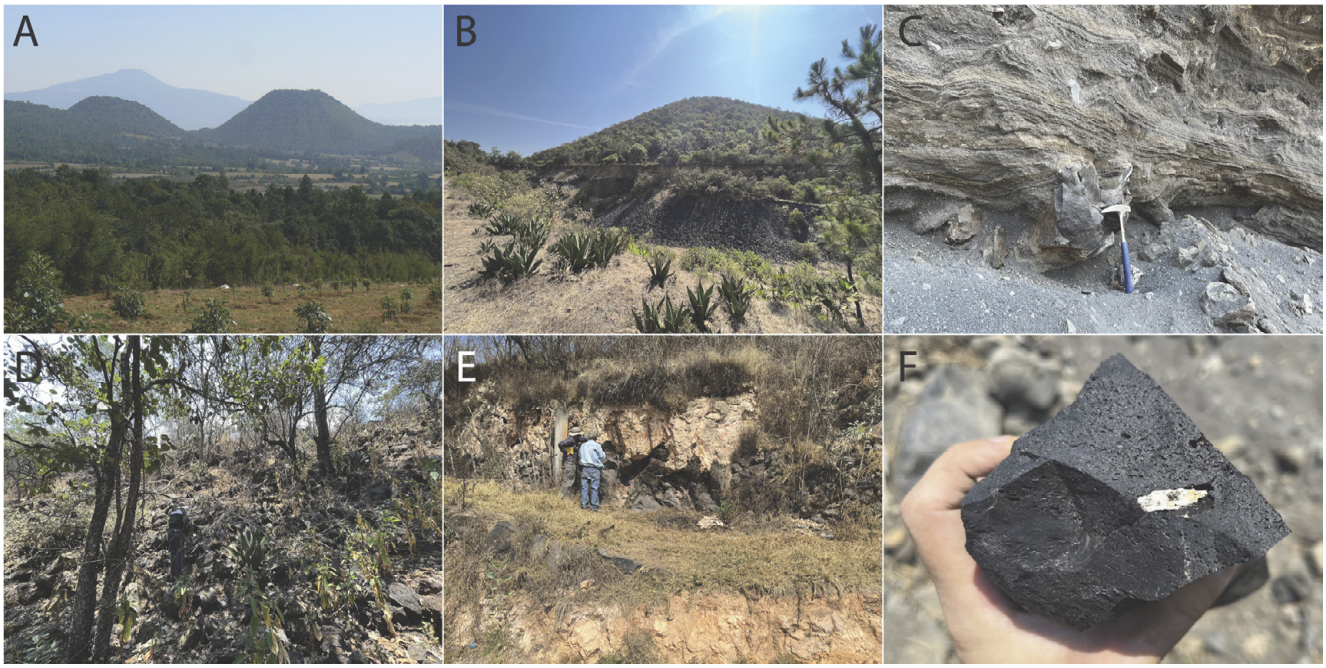

Figure 3: [A] La Taza scoria cone (right) seen from the south, [B] La Taza scoria cone seen from the base of Cerro Chendanas to the south with proximal tephra deposit at the base of the cone, [C] La Taza proximal tephra deposit showing multiple glassy bombs, [D] Typical La Taza lava flow front outcrop, blocky and heavily vegetated, [E] La Taza lava flow deposit (black) overlain by lake sediment deposits, [F] typical La Taza lava sample, black and aphanitic to slightly vitric. Sample contains a typical granitic xenolith, occasionally found in some lava samples.

the QGIS raster calculator to estimate the volume of the La Taza lava flows [Chevrel et al. 2016b; Ramírez-Uribe et al. 2021] (Figure 5C,5D).

The two most well-defined flows (Flow 2 and 4; Figure 6) were analyzed in detail using the DTM to obtain individual flow volume measurements, as well as to note other important characteristics (e.g. flow channel morphology, breakout areas). The number of flows chosen for study was selected following similar studies conducted on monogenetic volcanoes in the MGVF, for which between one and four flows per volcano were analyzed [Chevrel et al. 2016a; Ramírez-Uribe et al. 2021; Reyes-Guzmán et al. 2021]. We analyzed two flows at La Taza, following the Ramírez-Uribe et al. [2021] study of Rancho Seco, due to its similarity in size and number of lava flows (7), relative to the generally larger or smaller volcanoes in the other two studies. Measurements were obtained by taking ten elevation profiles perpendicular to the flow direction, as well as a profile parallel to flow direction (with each profile consisting of the average of five 1-m-spaced profiles in that location), which allowed for the measurement of flow length, width, channel width, thickness, and slope angle [Chevrel et al. 2016b; Ramírez-Uribe et al. 2021; Reyes-Guzmán et al. 2021] (Figure 6).

3.2 Petrography and geochemistry

Analysis of the DTM informed sampling for geochemical and petrological studies. Samples were collected from each lava flow front (at least one per flow). Additionally, tephra samples were taken from the top, middle, and bottom of the La Taza tephra sequence, and, where available, bombs were collected from proximal tephra deposits. Sample locations are visible on Figure 7 and coordinates are provided in Supplementary Material 2.

Representative thin-sections were created for all flows, tephra, and bomb samples. These were analyzed with a petrographic microscope to identify the major mineral phases. Modal mineralogy of the lava flow samples was obtained by counting 1000 points per sample at regular intervals, with points falling into the categories of plagioclase, orthopyroxene, clinopyroxene, hornblende, olivine, and quartz [Ramírez-Uribe et al. 2021]. Minerals were divided based on size into phenocrysts (>0.3 mm), microphenocrysts (<0.3 to 0.15 mm), and microlites (<0.15 mm), groundmass, and vesicles.

Whole rock samples were analyzed for major and trace elements using X-ray fluorescence. Analysis was done at Activation Laboratories Ltd. in Ancaster, Canada by fusion-inductively coupled plasma (FUS-ICP), total-digestion inductively coupled plasma (TD-ICP), and multi-instrumental neutron activation analysis (INAA). Details on methods used for each element and results of standard measurements showing measurement precision can be found in the full dataset (Supplementary Material 2).

Quantitative elemental analysis of mineral and glass phases for select samples was undertaken using a JEOL JXA-8230 Superprobe at the Microanalysis Laboratory of Instituto de Geofisíca, UNAM, Campus Morelia (Supplementary Material 3). The measuring conditions were an accelerating voltage of 15 kV and a beam current of 10 nA (with a diameter of 1 µm), and the counting times were 40 s for Ti, Fe, and Mg, and 10 s for K, Na, Ca, Si, and Al. Element measurements

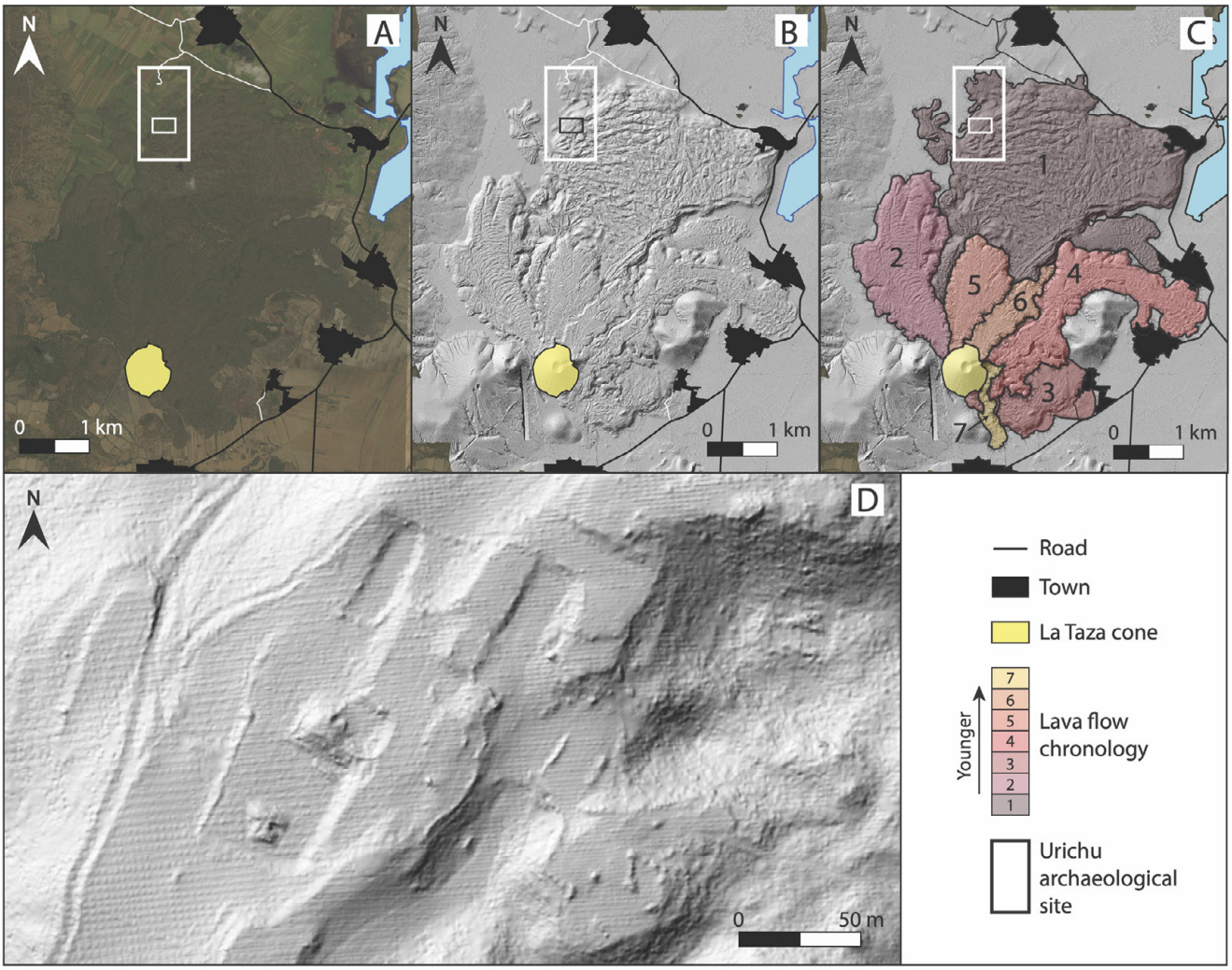

Figure 4: Maps showing the effectiveness of LiDAR imagery for studying the La Taza lava flows. Larger white box in [A]–[C] highlights the location of the Urichu archaeological site. The smaller box within denotes the area displayed in [D]. [A] Google Earth satellite imagery of La Taza and its flows, showing no visibility of flow morphology due to tree cover, [B] LiDAR DTM of La Taza and its flows, showing clear lava flow morphology, [C] LiDAR DTM of La Taza and its lava flows with flow field divided into individual flows, [D] detailed view of part of the Urichu archaeological site demonstrating the resolution of the LiDAR data.

were calibrated from a variety of reference mineral standards: PETL for Ti and Cr, LIFL for Mn, LIF for Fe, PETJ for K and Ca, and TAP for Na, Si, Al, and Mg. In addition, backscattered electron (BSE) images were obtained to observe details of the different mineral phases that could not be seen under the polarizing microscope.

3.3 Lava temperature, viscosity, and mean effusion rate

Empirically derived mineral thermometers, hygrometers, and barometers were used to calculate lava crystallization temperatures and pressures. Based on the mineral content of the La Taza lavas, we selected the plagioclase-liquid and orthopyroxene-liquid thermometers [Putirka 2008] as the most appropriate for calculating temperatures. For the plagioclase-liquid thermometer, a pressure of 1 kbar was used—this was based on the pressure associated with plagioclase-free andesites in the Zitácuaro area of eastern Michoacán [Blatter and Carmichael 1998], whose composition is similar to lava from comparable volcanoes in the MGVF (Rancho Seco [Ramírez-Uribe et al. 2021]). To estimate water content, we used a plagioclase hygrometer [Waters and Lange 2015]. For the plagioclase phase, temperature, and H_2O content were calculated iteratively using the `Thermobar` software developed by [Wieser et al. 2022]. These results were used together with the orthopyroxene-liquid barometer [Putirka 2008] to calculate syn-eruptive pressures. All methods involve standard equilibrium tests carried out in the `Thermobar` program to remove invalid results.

Calculations for viscosity involved the determination of liquid (η_{liq}), relative (η_r), and apparent (η_{app}) viscosity. Liquid viscosity was calculated for pre-and syn-eruptive conditions using the composition and water content of the lava samples following the formulas of [Giordano et al. 2008]. Calculations for pre-eruptive η_{liq} assumed the absence of crystals and used the whole rock geochemistry of each lava along with the temperature, pressure, and H_2O content calculated previ-

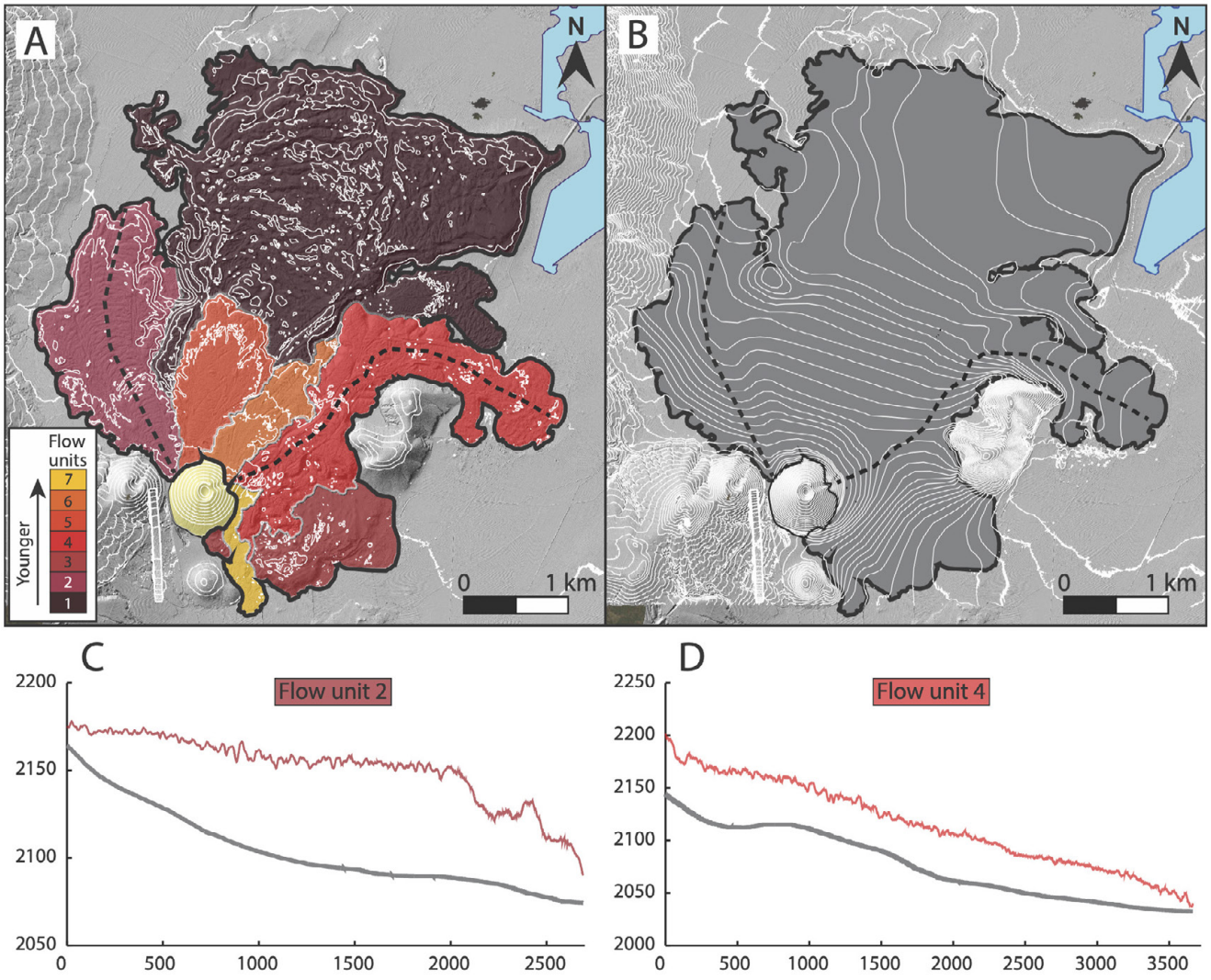

Figure 5: Maps demonstrating the use of interpolated pre-eruption topography to determine lava flow volume. [A] La Taza lava flows showing contours representing current topography, [B] contours showing extrapolated pre-eruption topography, [C]–[D] comparison of modern and pre-eruption topography for individual flows. Upper red line shows topographic profile for lava flows, lower gray line shows profile for pre-eruption topography.

ously. Calculations for syn-eruptive η_{liq} used glass compositions from a bomb collected from the proximal La Taza tephra sequence and an H_2O content of 0.1 wt.% (representing low water content due to assumed gas exsolution at the moment of eruption). Relative viscosity for each lava was obtained using the procedure of [Costa et al. 2009] and the measurements of [Cimarelli et al. 2011] to account for the crystal content of the La Taza lavas. This involved determining the proportion of spherical and prolate crystals based on the modal mineralogy. This approach is derived from the analysis of Rancho Seco volcano [Ramírez-Uribe et al. 2021]. The apparent viscosity at the time of eruption for each lava was determined using the equation $\eta_{app} = \eta_{liq} \times \eta_r$ [Chevrel et al. 2013].

The mean effusion rates, flow velocity, and duration of the eruption and lava flows were determined by analyzing the best exposed lava flows (Flows 2 and 4). Two types of methods were used to obtain estimates for these two flows: a "petrologic method," which considers the calculated apparent viscosity based on sample petrology together with some morphological characteristics, and two "morphological methods," which consider just the measured morphological features of the flows. The petrologic method uses the previously calculated viscosity in combination with some morphological characteristics as variables in the Jeffreys Equation [Jeffreys 1925] to calculate the flow velocity, which is then used to calculate the mean effusion rate and flow duration based on the flow volumes. The morphological methods used are the Grätz-Number method [Pinkerton and Sparks 1976; Hulme and Fielder 1977] and the Kilburn and Lopes [Kilburn and Lopes 1991] method, which both use measured morphological characteristics to calculate the mean effusion rate, velocity, and flow duration. These values can then be extrapolated to the full flow field by considering the total volume of the entire eruption. More details on the methods from Section 3.3 can be found in Supplementary Material 4. Note that definitions of "mean effusion rate" and "mean output rate" are used fol-

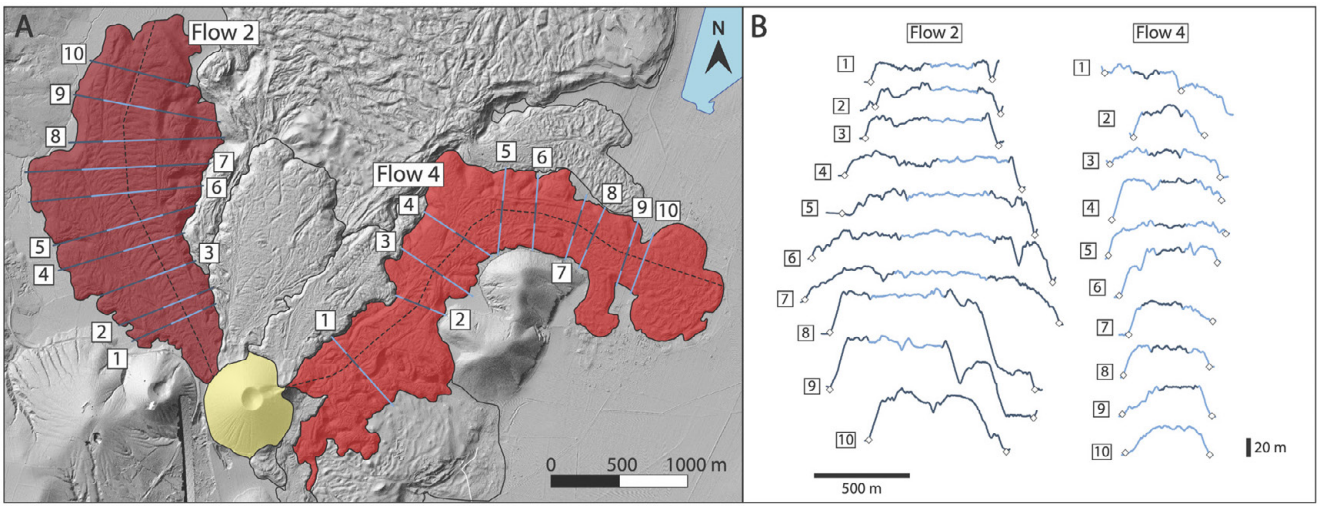

Figure 6: Morphological measurements for Flows 2 and 4. [A] Map highlighting Flows 2 and 4, blue lines show locations of cross sections, different color in center of each cross section represents the channel width. Dashed black lines represent flow paths along the center of the channel. [B] Cross sections of Flows 2 and 4, used to measure flow and channel width and thickness. Diamonds represent the points used to represent the base of the flows.

lowing those described in [Harris et al. 2007], in which mean effusion rate refers to effusion rate averaged over a specified period of time (e.g. a single lava flow) and mean output rate refers to the effusion rate averaged over the duration of an entire eruption.

Throughout the article, variation of measured values (e.g. morphological measurements) are presented as standard deviation, whereas uncertainty of calculated values (e.g. volumes, rates, velocities, etc.) are presented as percentage error obtained through propagation of uncertainty [Lefler 2011; Chevrel et al. 2016a; Ramírez-Uribe et al. 2021; Reyes-Guzmán et al. 2021].

4 Results

4.1 Flow morphology

The La Taza lava deposits consist of a sequence of seven individual flows of varying size and length (Figure 7). Based on interactions visible on the LiDAR DTM and in outcrops, it was possible to chronologically order the lava flows from oldest to most recent. Some lava flows are clearly overlapped by more recent ones, which means the true size of every flow is not possible to determine. It should be noted that some flows (e.g. Flow 1 and 3) do not share a direct contact, leaving their relationship more open to interpretation. Our map presents the most probable chronology based on the described methodology. The decision to select Flows 2 and 4 for more detailed analysis was also guided by the relative certainty about their relationship with the other flows. The lavas are black to grey and aphanitic, with some flows appearing more vitric. No crystals are visible at the hand sample scale. The lavas rarely contain granitic xenoliths which represent crustal assimilation during magma ascent [Corona-Chávez et al. 2006].

The lava flows reach 4.5 km from the cone at the furthest point to the north. The area covered by individual flows (as visible on the LiDAR map) ranges from 0.24 (Lava 7) to 7.6 km^2 (Lava 1; this value represents the minimum area of the largest flow, which is covered significantly by the younger flows). The total area of the flow field is approximately 15 km^2. For several flows, the flow channels and levees are clearly defined on the DTM and can be measured independently from the flow width. Lavas in the flow channel show ridges perpendicular to flow direction [Fink 1980], which could be used to interpret the flow path of some individual flows.

Detailed measurements of the flow parameters of Flow 2 give a flow distance of 2.2 km, average thickness of 40 m, average total flow and channel widths of 937 and 357 m, respectively, and slope angle of 1.9° (Table 1). Detailed measurements of the flow parameters of Flow 4 give a flow distance of 3.4 km, average thickness of 30 m, average total flow and channel widths of 508 and 190 m, respectively, and slope angle of 3.8° (Table 1).

Based on these parameters, the volume of Flow 2 is 8.2×10^7 m^3 and the volume of Flow 4 is 5.2×10^7 m^3. We used the previously described method of subtracting pre-eruption topography from the current topography to obtain a volume of 0.6 km^3 for the whole flow field. The full description of flow parameters and individual profile measurements can be found in Supplementary Material 5.

4.2 Geochemistry and petrology

Petrological analysis of thin-sections confirms the aphanitic texture of the lavas, with the plagioclase microlites showing a trachytic texture (Figure 8A). Phenocrysts are extremely rare (<4.4 vol.%) with most of the lavas comprised of microphenocrysts and microlites (28–60 vol.%) and groundmass (35–69 vol.%) (Figure 8B). A wide range of vesicularity is represented, ranging from 1 to 21 vol.% (with an average of 9.2 vol.% across all samples). The main mineral phases and modal mineralogies (normalized to 100 % to represent dense rock equivalent) seen in thin-section are plagioclase (26–56 vol.%), orthopyroxene (2–10 vol.%), clinopyroxene (0.3–5 vol.%), olivine

Table 1: Lava flow parameters from morphological measurements

Parameter	Unit	Flow 2	stdev	Flow 4	stdev
Flow width (W)	m	937	243	485	83
Channel width (w)	m	357	100	190	33
Length (L)	m	2202	2	3398	4
Thickness (H)	m	40	16	29	5
Slope (θ)	°	1.9	0.02	3.8	0.02
			error (%)		error (%)
Area*	m^2	2.06×10^6	5	1.65×10^6	4
Volume†	m^3	8.17×10^7	20	4.80×10^7	14

* Area = $L \times W$
† Volume = $L \times W \times H$

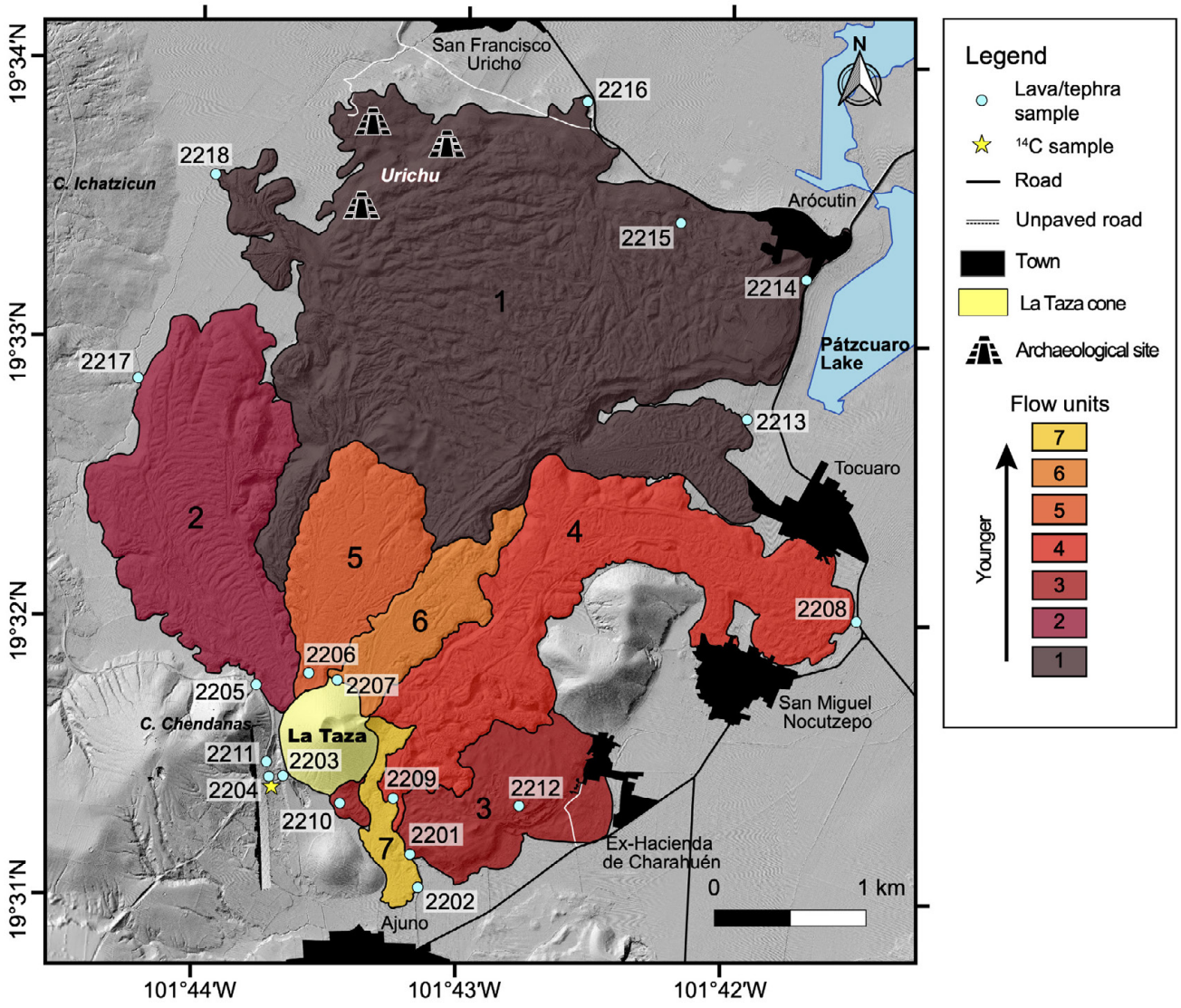

Figure 7: Map of La Taza scoria cone and its lava flows. The chronological order of the lava flows is marked by color and number. Urichu archaeological site is marked at the north end of Flow 1. Samples taken for geochemical and petrological studies and radiocarbon dating (PAZ-1202) in this study are marked.

(0.1–2.3 vol.%), oxides (0.5–4.2 vol.%), and groundmass (35–69 vol.%) (Figure 8C, 8D). Rare granitic xenolith phenocrysts were observed (0.3 vol.% in just two samples). Plagioclase crystals are typically needle-like or tabular in habit. Oxide minerals appear primarily as microlites and also occur as inclusions in olivines and rarely in larger pyroxene crystals. Orthopyroxenes are subhedral-euhedral in habit and represent the most common mineral phase apart from plagioclase both in phenocryst and microphenocryst/microlite size. Full modal mineralogy can be seen in Supplementary Material 6.

The whole rock geochemistry confirms the andesitic composition of the La Taza lavas (SiO_2: 57.6–63.0 wt.%), with all lava sample geochemistry (n = 14) falling within the andesitic range of the total alkali vs. silica diagram (Figure 9), showing some variation in silica without a clear trend. The variation in various elemental contents (e.g. K_2O: 1.5–2.0 wt.%, CaO: 5.6–6.8 wt.%, Fe_2O_3: 5.9–7.2 wt.%) is consistent with many other monogenetic volcanoes in the broader TMVB [Siebe et al. 2004] and also the MGVF [Cebriá et al. 2011; Larrea et al. 2019b], though there are some otherwise comparable volcanoes in the MGVF which show much more homogeneity in composition (e.g. Rancho Seco [Ramírez-Uribe et al. 2021]). Full whole rock compositional data can be seen in Supplementary Material 2.

Mineral and glass phase geochemistry was analyzed for 14 samples representing all seven flows and one bomb from within the tephra deposit (Supplementary Material 6). Results were obtained for rims of plagioclase, orthopyroxene, clinopyroxene, olivine, and glass phases. Only plagioclase and orthopyroxene rims returned enough valid results to proceed with further measurements (phase measurements with totals between 98 and 102 % were used). La Taza plagioclases fall under the labradorite classification (Figure 10A), while La Taza orthopyroxenes classify as enstatites (Figure 10B).

4.3 Thermobarometry, hygrometry, barometry

The plagioclase-liquid thermometer suggests magma temperature of 1070–1109 °C (±36 °C), while the orthopyroxene-liquid thermometer suggests magma temperatures of 1109–1129 °C (±39 °C). This results in an average magma temperature of 1102 °C. The orthopyroxene-liquid barometer suggests a pre-eruptive pressure range of 0.8–2.1 kbar (±2.6 kbar). The plagioclase-liquid hygrometer suggests a pre-eruptive water content of 0.9–1.7 wt.% (±0.35 wt.%). The full range of properties for each lava flow can be seen in Table 2 and 3.

4.4 Magma rheology

For pre-eruptive conditions, we estimated the liquid viscosity of the magma (estimated from bulk rock composition without crystals) at 3.6×10^2 to 1.5×10^3 Pa·s (1092–1119 °C, 0.9–1.7 wt.% H_2O; Table 4) following [Giordano et al. 2008]. The liquid viscosity of extruded lava was estimated at 2.3×10^5 to 4.2×10^5 Pa·s (1092—1119 °C, 0.1 wt.% H_2O; Table 4), considering the evolved melt phase composition (interstitial glass).

Relative viscosities for the lavas were calculated to be 1.9×10^2 to 3.0×10^3 based on the relative content of prolate (e.g. plagioclase) and spherical (e.g. pyroxene and olivine) crystals, following the methods of [Costa et al. 2009] with a deformation rate of 1 s^{-1} based on [Cimarelli et al. 2011], who determined the value from analogous experiments of polydisperse suspensions containing large, equant, and small, prolate particles in a bubble-free Newtonian liquid (which is analogous to interstitial silicate melt).

Using these values, the apparent viscosity across all extruded lavas at the time of eruption was calculated to be 5.4×10^8 Pa·s, with a range from 7.0×10^7 to 1.2×10^9 Pa·s. Full details of viscosity calculations can be found in Supplementary Material 7.

4.5 Mean effusion rate and emplacement duration

The morphological parameters (Table 1) and the viscosity calculated using petrological methods (Section 4.4) were used to determine the characteristics of the La Taza eruption (Table 5). For the petrological method, the apparent viscosities, the slope angles, average flow thicknesses for Flow 2 (1.2×10^9 Pa·s, 1.9°, 40 m) and Flow 4 (6.0×10^8 Pa·s, 3.8°, 30 m) were used along with the value for gravity (9.81 m s^{-2}) to calculate the flow velocity using the Jeffreys equation [Jeffreys 1925], resulting in velocities of 31 and 67 m day^{-1} for Flows 2 and 4, respectively. These velocities were used, together with the flow volumes, to calculate mean effusion rates of 13 and 11 m^3 s^{-1} and flow emplacement durations of 71 and 51 days for Flows 2 and 4, respectively.

The Grätz-Number method uses the flow length, width, and thickness, along with a constant Grätz-Number (300) and thermal diffusivity (4.21×10^{-7} m^2 s^{-1} [Kilburn and Lopes 1991]), to obtain the mean effusion rate. The mean effusion rate for Flow 2 (6 m^3 s^{-1}) and Flow 4 (7 m^3 s^{-1}) were used to obtain velocities (15 and 44 m day^{-1}) and emplacement durations (147 and 84 days) for the two flows.

The Kilburn and Lopes [1991] method used flow length, width, thickness, and slope angle, along with thermal diffusivity, to determine the emplacement duration of a lava flow. Emplacement durations for Flow 2 (201 days) and Flow 4 (83 days) were used to determine the velocities (11 and 51 m day^{-1}) and the mean effusion rates (5 and 8 m^3 s^{-1}) for the two flows.

The average mean effusion rates between the two flows, combined with the total volume of the La Taza eruption, were used to obtain estimates of the emplacement duration of the full eruption for each of the three methods: the petrological method has an estimate of 1.6 years for the full eruption, while the Grätz-Number and Kilburn and Lopes [1991] methods show eruption durations of 2.8 and 2.9 years, respectively. When accounting for uncertainty obtained by error propagation (which ranges between 20 and 73 % across all flows and methods for emplacement duration), the eruption had a minimum duration of 1.1 years and a maximum duration of 4.3 years.

5 Discussion

The eruption of La Taza scoria cone began with an initial Strombolian phase, evidenced by thin tephra fall deposits identified mostly in areas close to the volcano. This Strombolian phase was likely similar to that of Paricutin, in which

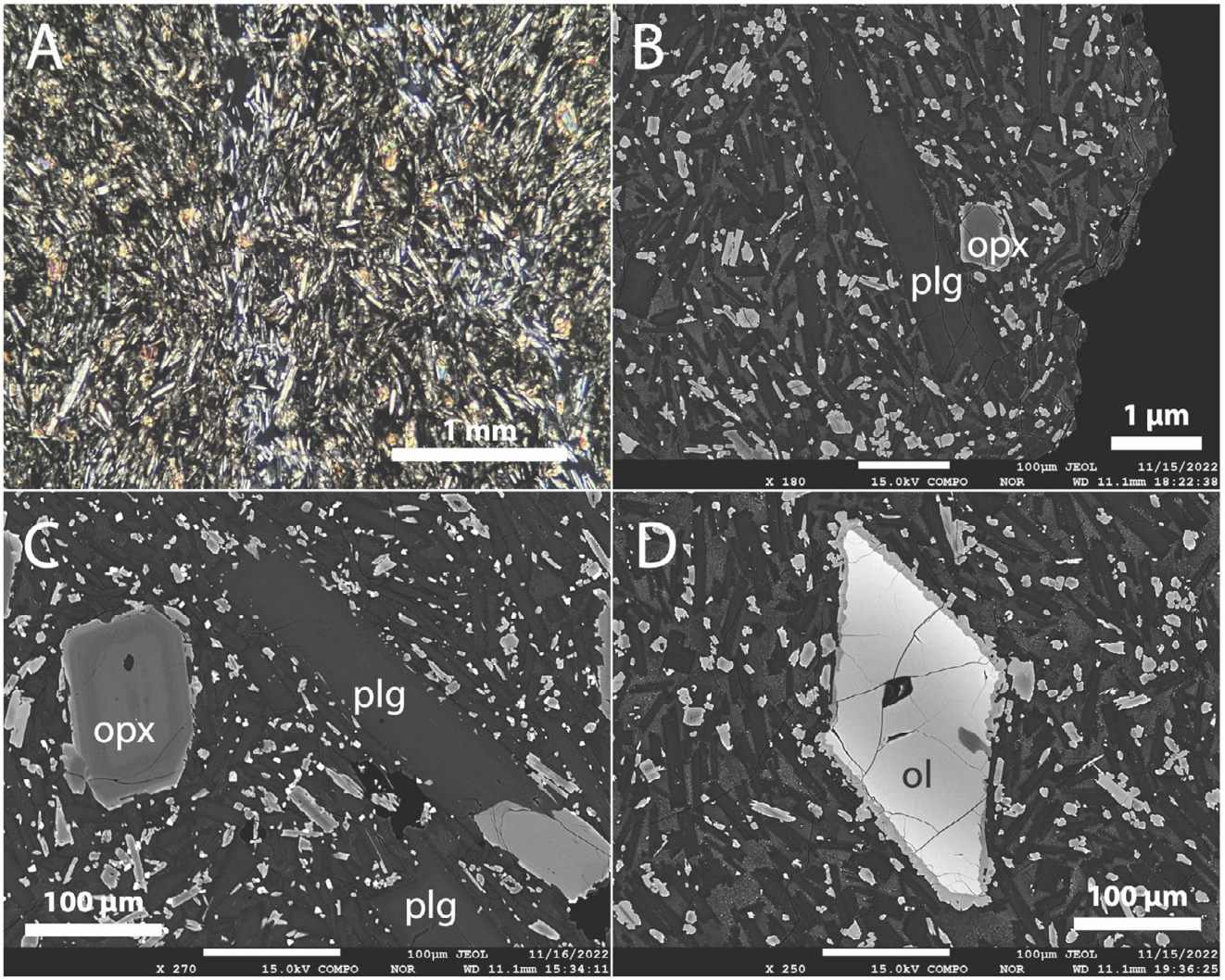

Figure 8: [A] Optical microscope photo under crossed polars at low magnification showing representative texture and fine grain-size of most mineral phases, with plagioclase microlites and groundmass representing the most common phases. [B]–[D] BSE images showing representative mineral phase compositions. Larger (microphenocryst-size) crystals are labeled, showing occasional plagioclase, orthopyroxene, and olivine phases. Microlites surrounding the larger crystals are primarily plagioclase (dark) and orthopyroxene (light), with some glass.

Table 2: Plagioclase-liquid thermometer and hygrometer results (Wieser et al. [2022] iterative method using Putirka [2008]; eq. 24a and Waters and Lange [2015]).

Sample(s)	Flow unit	n	Liquid comp	T (°C)	stdev	P (kbar)	wt.% H_2O	stdev
2216A, 2218	1	15 (Rim)	Whole rock	1080	12.2	1.0	1.7	0.05
2205, 2217	2	5 (Rim)	Whole rock	1071	4.4	1.0	1.6	0.11
2210, 2212	3	6 (Rim)	Whole rock	1089	13.2	1.0	1.5	0.05
2208	4	5 (Rim)	Whole rock	1070	2.1	1.0	1.6	0.02
2206	5	4 (Rim)	Whole rock	1078	8.8	1.0	1.4	0.19
2207	6	4 (Rim)	Whole rock	1098	3.5	1.0	1.1	0.01
2202A	7	4 (Rim)	Whole rock	1109	4.7	1.0	0.9	0.10

most of the cone (by volume) was built within a few weeks [Luhr and Simkin 1993]. While Strombolian activity continued over the years with ups and downs, it was simultaneous to lava flow emplacement [Luhr and Simkin 1993] and did not meaningfully impact the eruption duration. At La Taza, this phase was followed by the effusive phase that formed the lava field to the north of the volcano. This effusive phase consisted of seven lava flows of varying sizes emplaced in the

Table 3: Orthopyroxene-liquid thermometer and barometer results (Putirka [2008]; Eq. 28a and 29b).

Sample(s)	n	Liquid comp	T (°C)	stdev	P (kbar)	stdev
2218	3 (Rim)	Whole rock	1119	4.4	1.1	0.5
2205, 2217	19 (Rim)	Whole rock	1118	4.8	1.4	0.7
2210	6 (Rim)	Whole rock	1109	23.1	1.5	0.8
2208	7 (Rim)	Whole rock	1114	12.5	1.5	1.0
2206	11 (Rim)	Whole rock	1116	8.6	1.6	1.0
2207	3 (Rim)	Whole rock	1129	15.6	2.1	1.6
2202A	6 (Rim)	Whole rock	1129	12.2	0.8	0.5

Table 4: Magma and lava viscosities estimated using the petrological approach.

Sample(s)	Flow	Pre-eruptive conditions			Syn-eruptive conditions (0.1 wt.% H_2O)			
		T (°C)	wt.% H_2O	Melt viscosity (Pa·s)	T (°C)	Liquid viscosity (Pa·s)	Relative viscosity	Lava viscosity (Pa·s)
2216A, 2218	1	1100	1.7	3.6×10^2	1100	3.6×10^5	2.3×10^3	8.0×10^8
2205, 2217	2	1095	1.6	8.9×10^2	1095	4.0×10^5	3.0×10^3	1.2×10^9
2210, 2212	3	1099	1.5	5.1×10^2	1099	3.6×10^5	1.1×10^3	3.9×10^8
2208	4	1092	1.6	1.2×10^3	1092	4.2×10^5	1.4×10^3	6.0×10^8
2206	5	1097	1.4	1.5×10^3	1097	3.8×10^5	1.9×10^2	7.0×10^7
2207	6	1114	1.1	8.3×10^2	1114	2.6×10^5	2.5×10^3	6.6×10^8
2202A	7	1119	0.9	8.9×10^2	1119	2.3×10^5	3.7×10^2	8.5×10^7

Table 5: La Taza lava flow and eruption parameters.

	Jeffreys equation*		Grätz-Number†		Kilburn and Lopes [1991]‡	
	Flow 2	Flow 4	Flow 2	Flow 4	Flow 2	Flow 4
Velocity (m day^{-1})	31	67	15	44	11	51
Error (%)	*35*	*22*	*31*	*34*	*79*	*53*
Mean effusion rate (m^3 s^{-1})	13	11	6	7	5	8
Error (%)	*35*	*22*	*72*	*34*	*60*	*36*
Emplacement duration (days)	71	51	147	84	201	73
Error (%)	*40*	*26*	*73*	*37*	*40*	*20*
	Mean of Flows 2 and 4					
Mean effusion rate (m^3 s^{-1})	12		7		7	
	Full eruption (Flows 1–7)					
Emplacement duration (years)**	1.6 ± 0.5		2.8 ± 1.5		2.9 ± 0.9	

* Calculates flow velocity from density, gravity, flow depth, slope angle, and viscosity, which is used to calculate mean effusion rate and emplacement duration;
† Calculates mean effusion rate from Grätz-Number, thermal diffusivity, flow length, and flow depth, which is used to calculate velocity and emplacement duration;
‡ Calculates emplacement duration from flow width, flow depth, slope angle, thermal diffusivity, and flow length, which is used to calculate velocity and mean effusion rate;
** Calculated using total eruption volume from GIS method and the average of the mean effusion rate of Flows 2 and 4.

sequence indicated in Figure 7. While it is impossible to say for certain if all flows were emplaced sequentially (with or without a hiatus in activity between flows) or if some were emplaced contemporaneously, cross-cutting relationships visible in the LiDAR imagery combined with the fact that many of the flows are geochemically distinct from the immediately preceding/following flow indicate that most of the flows in the sequence probably began after the previous one had already been emplaced. There is no evidence for any further Strombolian activity following the end of the effusive phase of the eruption.

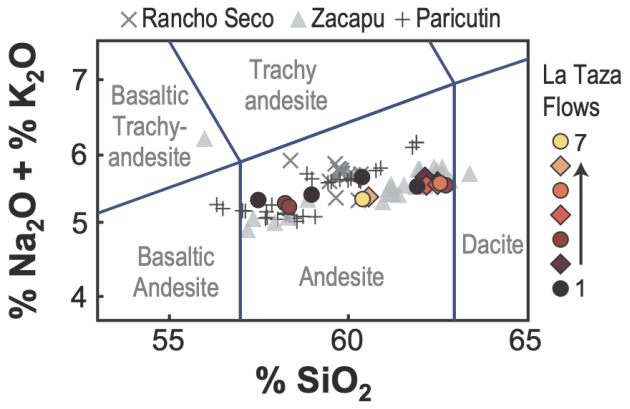

Figure 9: Total alkali vs. silica diagram [LeBas et al. 1986] for La Taza lavas with compositions from three other MGVF volcanic areas for comparison: Rancho Seco [Ramírez-Uribe et al. 2021], Malpaís de Zacapu [Reyes-Guzmán et al. 2021], and Paricutin [Cebriá et al. 2011; Larrea et al. 2019b].

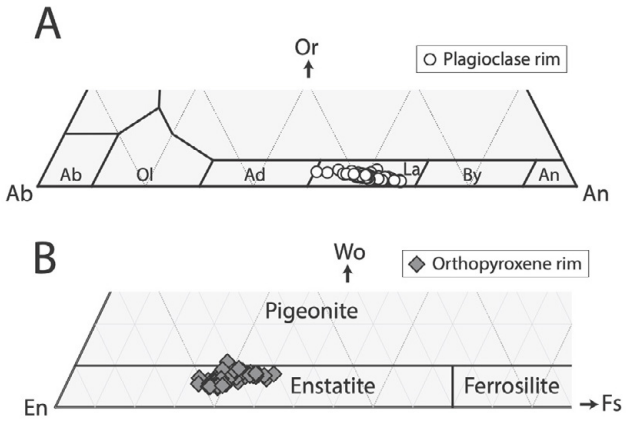

Figure 10: [A] Feldspar classification diagram, showing the composition of La Taza plagioclase phases used for temperature, pressure, and H_2O calculations. Plagioclases fall into the labradorite classification. [B] Pyroxene classification diagram, showing the composition of La Taza orthopyroxene phases used for temperature and pressure calculations. Orthopyroxenes fall primarily into the enstatite classification.

The seven lava flows vary widely in size, with the smallest, Flow 7, covering an area of 0.24 km^2 and the largest, Flow 1, covering at least 7.5 km^2 (it is partially covered by younger flows). The two flows studied in detail in this study, Flow 2 and 4, fall within this range, covering 2.1 and 1.7 km^2, respectively. Despite different dimensions, the calculated mean effusion rates for each flow were relatively similar within each of the three methods. Therefore, assuming a similar mean effusion rate for most flows, the volume of each flow would have a significant impact on the emplacement duration. A rough calculation obtained by using the mean effusion rates calculated in both morphological methods (7 m^3 s^{-1}) and the average height between Flows 2 and 4 (35 m) suggests the emplacement time for the individual La Taza lava flows likely ranged between 14 and 434 days (accounting for the same large error applied to the other emplacement duration calculations).

The compositions of the La Taza flows are all andesite, and the flows from the full eruption show a relatively larger range in SiO_2 (57.6–63 wt.%) than most other studied MGVF monogenetic eruptions (~5 wt.% compared to a typical range of ~2 wt.%) (Figure 9, Table 6). The closest compositional comparison to La Taza in the MGVF is El Metate (57–62 wt.% SiO_2), with Rancho Seco showing a similar median composition, albeit over a smaller range (58.5–60.6 wt.% SiO_2) [Chevrel et al. 2016a; Ramírez-Uribe et al. 2021]. The other MGVF eruptions showing the widest SiO_2 range are Paricutin [Larrea et al. 2017], El Astillero/El Pedregal [Larrea et al. 2019a; 2023], and El Metate [Chevrel et al. 2016a]. Since these three eruptions represent the longest, shortest, and near-median lengths of studied MGVF eruptions, there is no clear connection between eruption duration and magma evolution during a monogenetic episode. At La Taza, there is no apparent temporal pattern in the geochemical evolution of the flows during the eruption sequence. Consecutive flows do not show a linear increase or decrease in SiO_2 content, with some of the older flows (e.g. Flow 1 and 3) showing a range of andesitic compositions within a single eruption (Figure 9), indicating possible new ascent of magma for each lava flow during the sequence. Since ascent of new magma leading to evolution in composition has been observed even within single eruptions [Kereszturi and Nmeth 2012], the wider variation in the SiO_2 of these two older flows could potentially indicate slower mean effusion rates, allowing more time for introduction of new magma during their eruption. This contrasts, for example, with Paricutin, in which the sequence of lava flows grew progressively more silica-rich over time [Larrea et al. 2017]. The presence of granitic xenocrysts in some La Taza lava samples (Figure 3F) similar to those found in other MGVF andesites [e.g. Luhr and Carmichael 1985; Corona-Chávez et al. 2006; Ramírez-Uribe et al. 2021] could indicate similar conditions of crystal fractionation and crustal assimilation during magma ascent.

Based on petrological analysis, La Taza flows show viscosities at the time of eruption on orders of magnitude between 10^7–10^9 Pa·s and a general but non-linear decrease through the emplacement sequence—Flow 1 has the highest viscosity, while Flow 7 has the second lowest viscosity (Table 4). Within the MGVF, calculated lava viscosities range between 10^4 and 10^{11} Pa·s (Table 6), with most volcanoes limited within two to three orders of magnitude of viscosity. Rancho Seco is the closest analogue for La Taza within the MGVF in terms of viscosity (10^8–10^9 Pa·s) [Ramírez-Uribe et al. 2021]. Calculations of viscosity at other andesite lava flows from stratovolcanoes in various parts of the world (Colima, Shinmodake, Lonquimay, Popocatépetl) have returned viscosities on the order of 10^6–10^{10} [Navarro-Ochoa et al. 2002; Sato et al. 2013; Castruccio and Contreras 2016; Ramírez-Uribe et al. 2022]. These examples share the characteristic of MGVF volcanoes of mostly having lava viscosities constrained to two to three orders of magnitude, except for Lonquimay, which showed a range of 10^6–10^9 Pa·s [Castruccio and Contreras 2016]. In all of these cases, calculated temperatures and viscosities represent the

Table 6: Comparison of eruption characteristics of MGVF effusive volcanic structures (sorted by minimum eruption duration).

MGVF volcano	Age	SiO_2 content (wt.%)	Lava viscosity order of magnitude (Pa·s)	Erupted volume (km^3)	Mean output rate ($m^3\ s^{-1}$)	Eruption duration (years)
El Astillero[a]	500–700 CE	52–57	-	0.12	~1	~0.5
Infiernillo[b,c]	3.2 ka BP	57–59	10^4–10^5	0.29	~14	~0.6
La Taza[d]	9400 ka BP	57.6–63	10^7–10^9	0.6	7–12	1.1–4.3
Rancho Seco[e,f]	27.8 ka BP	58.5–60.6	10^8–10^9	0.72	4–15	2–6
Malpais Prieto[c,g]	900 CE	61–63	10^4–10^6	0.51	5–6	2.5–3.1
Las Viboras[c,g]	3.2 ka BP	61–63	10^5–10^6	0.47	2–6	2.9–8.2
El Pedregal[a]	500–700 CE	58–60	-	0.46	1–35	~4.3
Parícutin[h,i]	1943–1952 CE	53–60.5	10^4–10^5	1.76	2–14	9
Jorullo[j,k]	1759–1774 CE*	52–55	-	0.35	~1	15*
Capaxtiro[b,c]	2.2 ka BP	62–63.5	10^5–10^6	3.10	~4	~27.1
El Metate[l]	1250 CE	57–62	10^9–10^{11}	9.20	12–60	35–275

[a] Larrea et al. [2019a]
[b] Reyes-Guzmán et al. [2018]
[c] Reyes-Guzmán et al. [2021]
[d] This study
[e] Ramírez-Uribe et al. [2019]
[f] Ramírez-Uribe et al. [2021]
[g] Mahgoub et al. [2018]
[h] Larrea et al. [2017]
[i] Larrea et al. [2019b]
[j] Rowland et al. [2009]
[k] Guilbaud et al. [2011]
[l] Chevrel et al. [2016a]
* Guilbaud et al. [2011] suggest the Jorullo eruption may have ended in 1766, meaning a duration of 7 years.

moment of eruption—at the time of emplacement, lavas would have a lower temperature and higher viscosity.

Characteristics of monogenetic eruptions within the MGVF studied in a similar level of detail are summarized in Table 6. Possible eruption durations within the MGVF range between 6 months (El Astillero) and 275 years (El Metate). When compared to the most similar monogenetic eruptions (<1 km^3 erupted volume), La Taza has one of the highest mean output rates. Combined with its relatively small volume, this means that La Taza had one of the shortest duration eruptions of all studied MGVF volcanoes. It should be noted that there are ~1400 volcanic vents within the MGVF, therefore there are certainly monogenetic eruption styles with characteristics that extend beyond the 11 well-studied eruptions discussed here (including more explosive phreatomagmatic eruptions [Hasenaka and Carmichael 1985]). El Metate is recognized as one of the largest shields within the MGVF [Chevrel et al. 2016a; b] and therefore represents a reasonable upper limit for eruption size and duration, whereas there are likely many eruptions within the MGVF with smaller eruption volumes and durations than those represented in Table 6. Studies of monogenetic eruption mean effusion rate and duration of this level of detail have primarily been conducted on MGVF volcanoes, therefore there are few global comparisons for which similar data is available. Two andesitic eruptions that have been studied in a similar fashion in other parts of the world include the well-observed 1988–1990 CE Lonquimay stratovolcano (Chile) lava flow, which extruded ~0.23 km^3 of material in ~13 months (average mean effusion rate of 7 $m^3\ s^{-1}$) [Naranjo et al. 1992] and the monogenetic ~1600 BP Collier Cone, which extruded ~0.17 m^3 of material in 255–275 days (mean output rate of 7–8 $m^3\ s^{-1}$) [Deardorff and Cashman 2012]. While much smaller in size, they display similar mean effusion rates to those obtained for La Taza using the morphological methods. It is also important to consider that in observed eruptions (e.g. Lonquimay, Paricutin), effusion rate at the start of the eruption is often up to an order of magnitude higher than the mean output rate across the entire eruption, dropping off significantly over time [Naranjo et al. 1992; Larrea et al. 2017], and the same was likely the case with La Taza.

Uncertainty in the calculated eruption duration (and other calculated characteristics such as velocity and mean effusion rate) are mostly similar to other attempts to constrain eruption characteristics at up to 40 %, though with few instances of significantly higher propagated error up to 79 % [e.g. Chevrel et al. 2016a; Reyes-Guzmán et al. 2021] obtained propagated errors up to and over 40 %, while [Ramírez-Uribe et al. 2021] obtained significantly lower propagated errors up to 15 %). These instances of particularly high propagated error occur when using the morphological methods (Grätz Number and [Kilburn

and Lopes 1991]), primarily due to the high variation in flow thickness measured at cross sections spanning the length of the flow, especially Flow 2, which has a standard deviation of flow thickness equal to 40 % of the measured value. This is a natural function of the variability of the flow thickness in a lava deposit, as noted by [Kilburn and Lopes 1991], [Chevrel et al. 2016a], and [Reyes-Guzmán et al. 2021]. Therefore, we believe that accounting for the large uncertainty by allowing for a range of emplacement durations, as done here and in other studies, is a more effective way to account for the uncertainty in eruption characteristics. Additionally, the derivation of the emplacement time range from multiple methods is important, as the petrological method can produce results that are quite different from the morphological methods [cf. Ramírez-Uribe et al. 2021]. The study of pre-historic lava flow sequences (including La Taza and most of the examples in Table 6) also involves the difficulty in accounting for the duration of the Strombolian phase, as well as any potential break in activity between lava flows or flows emplaced simultaneously. While the contribution of the Strombolian phase is generally negligible relative to the eruption durations seen in the MGVF, uncertainty due to the possibility of gaps in activity or concurrently emplaced flows should be considered when evaluating duration estimates. In the case of La Taza, it should be noted that in recent observed MGVF eruptions (Jorullo and Paricutin) effusive activity has been relatively constant through the eruption [Larrea et al. 2017].

Data about lava flow behavior and the duration of effusive monogenetic eruptions is valuable when planning for future eruptions within distributed volcanic fields. Two historic eruptions in Michoacán, Mexico had significant impacts on nearby populations, with the eruption of Jorullo (beginning in 1759 CE) and Paricutin (1943–1952 CE) destroying towns and agriculture close to the eruption sites [Gadow 1930; Wilcox 1954; Luhr and Simkin 1993; Guilbaud et al. 2009]. There is also evidence of older eruptions in Mexico having significant impacts on pre-Hispanic cultures (e.g. eruptions from Xitle volcano near present-day Mexico City and the Malpaís de Zacapu in Michoacán [Siebe 2000; Reyes-Guzmán et al. 2023]). The low velocity of the La Taza lava flows (maximum 67 m day^{-1}) and those from similar eruptions mean that there is minimal direct threat to human life from effusive hazards. However, the prolonged duration (up to over four years in the case of La Taza and tens to over a hundred years in the case of the longest-lasting studied MGVF eruption, El Metate [Chevrel et al. 2016a]) presents the potential for significant infrastructure, economic, and societal impacts. Recently, though not monogenetic (and not compositionally the same as most MGVF volcanoes), the eruptions of Kīlauea (Hawai'i) in 2018 [Meredith et al. 2022] and Cumbre Vieja (La Palma) in 2021 [Carracedo et al. 2022] show examples of the impact of prolonged effusive eruptions on inhabited areas (lasting about 4 and 3 months, respectively). Despite minimal casualties from the effusive phases of their activity, these eruptions led to the displacement of over 5500 and 6000 people and the destruction of over 1800 and 2800 structures, respectively [GVP 2022; Meredith et al. 2022]. A La Taza-style eruption lasting a minimum of a year taking place near an inhabited area would require long-term evacuation or relocation, resulting in a significant and prolonged impact on the livelihood and economy of the area. The better understanding of eruptions that have taken place within the MGVF across its entire period of activity allows for future hazard planning based on a range of potential eruption types and impacts beyond those observed historically at Jorullo and Paricutin and will hopefully contribute to an effective response in the event of a future eruption.

6 Conclusions

The eruption of the andesitic La Taza scoria cone around 8500–8200 ka BP represents one of the potential effusive eruption styles within the MGVF. This eruption consisted of a Strombolian phase followed by the emplacement of seven lava flows. Based on methods that account for the petrology of the La Taza lavas as well as the lava flow morphology (obtained in high precision using LiDAR data), the eruption lasted between about one and four years, making it one of the shorter eruptions that has been studied within the MGVF. Nonetheless, an eruption of this style and duration would present significant hazards if the vent in an expected future MGVF eruption is near enough to an inhabited area. At present, the vast majority of high-detail viscosity studies of this type have been undertaken at MGVF volcanoes. More morphological and petrological studies of lava and eruption characteristics at individual monogenetic volcanoes in other volcanic fields (in volcanic fields with varied compositions, sizes, and tectonic settings) would allow for better comparison and broader conclusions about monogenetic eruption styles.

Author Contributions

CS conceived the project. GAL wrote the first draft of the manuscript. IRU performed LiDAR mapping of lava flows and volume estimation. GAL, IRU, and CS undertook fieldwork and sample collection. GL performed all morphological, petrological, geochemical analyses and calculations with assistance from IRU and CS. CF provided the original LiDAR dataset along with input on archaeological matters. All authors contributed to the writing of the final manuscript.

Acknowledgements

The authors are grateful to Brett Carr, an anonymous reviewer, and Volcanica editor Alan Whittington for constructive comments that helped improve the manuscript. Funding for the project was provided by Dirección General de Asuntos del Personal Académico through project UNAM-DGAPA IN-104221. GAL was supported by the UNAM Posdoctoral Program (POSDOC). The authors thank Felipe García Tenorio for his work making the thin sections and Noemí Salazar Hermenegildo and Giovanni Sosa Ceballos for assistance with use of the microprobe. GAL is grateful to May Sas and Elizabeth Rangel-Granados for helpful discussions regarding geothermometry. CS benefitted from a sabbatical stay at the Senckenberg Naturhistorische Sammlungen, Dresden and the kind hospitality of Jan-Michael Lange and Peter Suhr.

Data Availability

Detailed data is available within the supplementary files associated with the manuscript.

Copyright notice

References

Blatter, D. L. and I. S. E. Carmichael (1998). "Plagioclase-free andesites from Zitácuaro (Michoacán), Mexico: petrology and experimental constraints". *Contributions to Mineralogy and Petrology* 132(2), pages 121–138. DOI: 10.1007/s004100050411.

Blatter, D. L. and L. Hammersley (2010). "Impact of the Orozco Fracture Zone on the central Mexican Volcanic Belt". *Journal of Volcanology and Geothermal Research* 197(1–4), pages 67–84. DOI: 10.1016/j.jvolgeores.2009.08.002.

Cappello, A., G. Ganci, S. Calvari, N. M. Pérez, P. A. Hernández, S. V. Silva, J. Cabral, and C. Del Negro (2016a). "Lava flow hazard modeling during the 2014–2015 Fogo eruption, Cape Verde". *Journal of Geophysical Research: Solid Earth* 121(4), pages 2290–2303. DOI: 10.1002/2015jb012666.

Cappello, A., A. Hérault, G. Bilotta, G. Ganci, and C. Del Negro (2016b). "MAGFLOW: a physics-based model for the dynamics of lava-flow emplacement". *Geological Society, London, Special Publications* 426(1), pages 357–373. DOI: 10.1144/sp426.16.

Carracedo, J. C., V. R. Troll, J. M. D. Day, H. Geiger, M. Aulinas, V. Soler, F. M. Deegan, F. J. Perez-Torrado, G. Gisbert, E. Gazel, A. Rodriguez-Gonzalez, and H. Albert (2022). "The 2021 eruption of the Cumbre Vieja volcanic ridge on La Palma, Canary Islands". *Geology Today* 38(3), pages 94–107. DOI: 10.1111/gto.12388.

Cashman, K. V., S. A. Soule, B. H. Mackey, N. I. Deligne, N. D. Deardorff, and H. R. Dietterich (2013). "How lava flows: New insights from applications of lidar technologies to lava flow studies". *Geosphere* 9(6), pages 1664–1680. DOI: 10.1130/ges00706.1.

Castruccio, A. and M. A. Contreras (2016). "The influence of effusion rate and rheology on lava flow dynamics and morphology: A case study from the 1971 and 1988–1990 eruptions at Villarrica and Lonquimay volcanoes, Southern Andes of Chile". *Journal of Volcanology and Geothermal Research* 327, pages 469–483. DOI: 10.1016/j.jvolgeores.2016.09.015.

Castruccio, A., A. C. Rust, and R. S. J. Sparks (2013). "Evolution of crust- and core-dominated lava flows using scaling analysis". *Bulletin of Volcanology* 75(1). DOI: 10.1007/s00445-012-0681-2.

Cebriá, J. M., B. M. Martiny, J. López-Ruiz, and D. J. Morán-Zenteno (2011). "The Parícutin calc-alkaline lavas: New geochemical and petrogenetic modelling constraints on the crustal assimilation process". *Journal of Volcanology and Geothermal Research* 201, pages 113–125. DOI: 10.1016/j.jvolgeores.2010.11.011.

Chase, A. F., D. Z. Chase, C. T. Fisher, S. J. Leisz, and J. F. Weishampel (2012). "Geospatial revolution and remote sensing LiDAR in Mesoamerican archaeology". *Proceedings of the National Academy of Sciences* 109(32), pages 12916–12921. DOI: 10.1073/pnas.1205198109.

Chevrel, M. O., C. Cimarelli, L. deBiasi, J. B. Hanson, Y. Lavallée, F. Arzilli, and D. B. Dingwell (2015). "Viscosity measurements of crystallizing andesite from <scp>T</scp> ungurahua volcano (<scp>E</scp> cuador)". *Geochemistry, Geophysics, Geosystems* 16(3), pages 870–889. DOI: 10.1002/2014gc005661.

Chevrel, M. O., M.-N. Guilbaud, and C. Siebe (2016a). "The ~AD 1250 effusive eruption of El Metate shield volcano (Michoacán, Mexico): magma source, crustal storage, eruptive dynamics, and lava rheology". *Bulletin of Volcanology* 78(4). DOI: 10.1007/s00445-016-1020-9.

Chevrel, M. O., H. Pinkerton, and A. J. Harris (2019). "Measuring the viscosity of lava in the field: A review". *Earth-Science Reviews* 196, page 102852. DOI: 10.1016/j.earscirev.2019.04.024.

Chevrel, M. O., T. Platz, E. Hauber, D. Baratoux, Y. Lavallée, and D. Dingwell (2013). "Lava flow rheology: A comparison of morphological and petrological methods". *Earth and Planetary Science Letters* 384, pages 109–120. DOI: 10.1016/j.epsl.2013.09.022.

Chevrel, M. O., C. Siebe, M.-N. Guilbaud, and S. Salinas (2016b). "The AD 1250 El Metate shield volcano (Michoacán): Mexico's most voluminous Holocene eruption and its significance for archaeology and hazards". *The Holocene* 26(3), pages 471–488. DOI: 10.1177/0959683615609757.

Cimarelli, C., A. Costa, S. Mueller, and H. M. Mader (2011). "Rheology of magmas with bimodal crystal size and shape distributions: Insights from analog experiments: Rheology of porphyritic magmas". *Geochemistry, Geophysics, Geosystems* 12(7). DOI: 10.1029/2011gc003606.

Connor, L. J., C. B. Connor, K. Meliksetian, and I. Savov (2012). "Probabilistic approach to modeling lava flow inundation: a lava flow hazard assessment for a nuclear facility in Armenia". *Journal of Applied Volcanology* 1(1). DOI: 10.1186/2191-5040-1-3.

Corona-Chávez, P., M. Reyes-Salas, V. H. Garduño-Monroy, I. Israde-Alcántara, R. Lozano-Santa Cruz, O. Morton-Bermea, and E. Hernández-Álvarez (2006). "Asimilación de xenolitos graníticos en el Campo Volcánico Michoacán-Guanajuato: el caso de Arócutin Michoacán, México". *Revista Mexicana de Ciencias Geológicas* 23, pages 233–245.

Costa, A., L. Caricchi, and N. Bagdassarov (2009). "A model for the rheology of particle-bearing suspensions and partially molten rocks". *Geochemistry, Geophysics, Geosystems* 10, Q03010. DOI: 10.1029/2008GC002138.

Deardorff, N. D. and K. V. Cashman (2012). "Emplacement conditions of the c. 1,600-year bp Collier Cone lava flow, Oregon: a LiDAR investigation". *Bulletin of Volcanology* 74(9), pages 2051–2066. DOI: 10.1007/s00445-012-0650-9.

Deligne, N. I., R. M. Conrey, K. V. Cashman, D. E. Champion, and W. H. Amidon (2016). "Holocene volcanism of the upper McKenzie River catchment, central Oregon Cascades, USA". *Geological Society of America Bulletin* 128(11–12), pages 1618–1635. DOI: 10.1130/b31405.1.

Dietterich, H. R. and K. V. Cashman (2014). "Channel networks within lava flows: Formation, evolution, and implications for flow behavior". *Journal of Geophysical Research: Earth Surface* 119(8), pages 1704–1724. DOI: 10.1002/2014jf003103.

Dietterich, H. R., D. T. Downs, M. E. Stelten, and H. Zahran (2018). "Reconstructing lava flow emplacement histories with rheological and morphological analyses: the Harrat Rahat volcanic field, Kingdom of Saudi Arabia". *Bulletin of Volcanology* 80(12). DOI: 10.1007/s00445-018-1259-4.

Fink, J. (1980). "Surface folding and viscosity of rhyolite flows". *Geology* 8, pages 250–254. DOI: 10.1130/0091-7613(1980)8<250:SFAVOR>2.0.CO;2.

Fisher, C. T. and S. J. Leisz (2013). "New Perspectives on Purépecha Urbanism Through the Use of LiDAR at the Site of Angamuco, Mexico". *Mapping Archaeological Landscapes from Space*. Edited by D. C. Comer and M. J. Harrower. SpringerBriefs in Archaeology. New York, NY: Springer, pages 199–210. DOI: 10.1007/978-1-4614-6074-9_16.

Fisher, C. T., A. S. Cohen, J. C. Fernández-Diaz, and S. J. Leisz (2017). "The application of airborne mapping LiDAR for the documentation of ancient cities and regions in tropical regions". *Quaternary International* 448, pages 129–138. DOI: 10.1016/j.quaint.2016.08.050.

Forest, M. (2020). "Architecture and urbanism at El Palacio". *El Palacio. Historiography and New Perspectives on a Pre-Tarascan City of Northern Michoacán, Mexico*. Edited by M. Forest. Monographs in American Archaeology. Paris: Archaeopress, pages 79–104.

Forest, M., L. Costa, and G. Pereira (2018). *Le collectif face au big data: interprétation partagée et retro-validation des données LiDAR du site d'El Infiernillo, Michoacán, Mexique*. URL: https://www.openscience.fr/Le-collectif-face-au-big-data-interpretation-partagee-et-retro-validation-des (visited on 04/05/2023).

Gadow, H. (1930). *Jorullo: The History of the Volcano of Jorullo and the Reclamation of the Devastated District by Animals and Plants*. CUP Archive.

García-Quintana, A., A. Goguitchaichvili, J. Morales, M. Cervantes-Solano, S. Osorio-Ocampo, J. L. Macias, and J. Urrutia-Fucugauchi (2016). "Datación magnética de rocas volcánicas formadas durante el Holoceno: caso de flujos de lava alrededor del Lago de Pátzcuaro (campo volcánico Michoacán-Guanajuato)". *Revista Mexicana de Ciencias Geológicas* 33, pages 209–220.

Giordano, D., J. K. Russell, and D. B. Dingwell (2008). "Viscosity of magmatic liquids: A model". *Earth and Planetary Science Letters* 271(1–4), pages 123–134. DOI: 10.1016/j.epsl.2008.03.038.

Global Volcanism Program (GVP) (2022). "Report on La Palma (Spain)". *Bulletin of the Global Volcanism Network*. Edited by E. Venzke. Volume 47. 2. Smithsonian Institution. DOI: 10.5479/si.gvp.bgvn202202-383010.

Gómez-Tuena, A., M. T. Orozco-Esquivel, and L. Ferrari (2005). "Petrogénesis ígnea de la Faja Volcánica Transmexicana". *Boletín de la Sociedad Geológica Mexicana* 57, pages 227–283. DOI: 10.18268/bsgm2005v57n3a2.

Griffiths, R. W. (2000). "The Dynamics of Lava Flows". *Annual Review of Fluid Mechanics* 32(1), pages 477–518. DOI: 10.1146/annurev.fluid.32.1.477.

Guilbaud, M.-N., C. Siebe, P. Layer, and S. Salinas (2012). "Reconstruction of the volcanic history of the Tacámbaro-Puruarán area (Michoacán, México) reveals high frequency of Holocene monogenetic eruptions". *Bulletin of Volcanology* 74(5), pages 1187–1211. DOI: 10.1007/s00445-012-0594-0.

Guilbaud, M.-N., C. Siebe, P. Layer, S. Salinas, R. Castro-Govea, V. H. Garduño-Monroy, and N. Le Corvec (2011). "Geology, geochronology, and tectonic setting of the Jorullo Volcano region, Michoacán, México". *Journal of Volcanology and Geothermal Research* 201(1–4), pages 97–112. DOI: 10.1016/j.jvolgeores.2010.09.005.

Guilbaud, M.-N., C. Siebe, C. Rasoazanamparany, E. Widom, S. Salinas, and R. Castro Govea (2019). "Petrographic, Geochemical and Isotopic (Sr–Nd–Pb–Os) Study of Plio-Quaternary Volcanics and the Tertiary Basement in the Jorullo-Tacámbaro Area, Michoacán-Guanajuato Volcanic Field, Mexico". *Journal of Petrology* 60(12), pages 2317–2338. DOI: 10.1093/petrology/egaa006.

Guilbaud, M.-N., C. Siebe, and S. Salinas (2009). *Excursions to Paricutin and Jorullo (Michoacán), the youngest volcanoes of the Trans-Mexican Volcanic Belt. A commemorative fieldtrip on the occasion of the 250th anniversary of Volcán Jorullo's birthday on September 29, 1759*. México, D.F.: Impretei S.A.

Harris, A. J. L. (2015). "Basaltic Lava Flow Hazard". *Volcanic Hazards, Risks and Disasters*. Elsevier, pages 17–46. ISBN: 9780123964533. DOI: 10.1016/b978-0-12-396453-3.00002-2.

Harris, A. J. L., J. Dehn, and S. Calvari (2007). "Lava effusion rate definition and measurement: a review". *Bulletin of Volcanology* 70(1), pages 1–22. DOI: 10.1007/s00445-007-0120-y.

Harris, E. (2019). "Viewed from above: Extracting the built environment from the ancient Purépecha site of Angamuco through development of a new methodology". Colorado State University.

Hasenaka, T. (1994). "Size, distribution, and magma output rate for shield volcanoes of the Michoacán-Guanajuato volcanic field, Central Mexico". *Journal of Volcanology and Geothermal Research* 63, pages 13–31. DOI: 10.1016/0377-0273(94)90016-7.

Hasenaka, T. and I. S. E. Carmichael (1985). "The cinder cones of Michoacán—Guanajuato, central Mexico: their age, volume and distribution, and magma discharge rate". *Journal of Volcanology and Geothermal Research* 25(1–2), pages 105–124. DOI: 10.1016/0377-0273(85)90007-1.

– (1987). "The Cinder Cones of Michoac n-Guanajuato, Central Mexico: Petrology and Chemistry". *Journal of Petrology* 28(2), pages 241–269. DOI: 10.1093/petrology/28.2.241.

Hayes, J. L., T. M. Wilson, N. I. Deligne, J. M. Lindsay, G. S. Leonard, S. W. Tsang, and R. H. Fitzgerald (2020). "Developing a suite of multi-hazard volcanic eruption scenarios using an interdisciplinary approach". *Journal of Volcanology and Geothermal Research* 392, page 106763. DOI: 10.1016/j.jvolgeores.2019.106763.

Hulme, G. (1974). "The Interpretation of Lava Flow Morphology". *Geophysical Journal International* 39(2), pages 361–383. DOI: 10.1111/j.1365-246x.1974.tb05460.x.

Hulme, G. and G. Fielder (1977). "Effusion rates and rheology of lunar lavas". *Philosophical Transactions of the Royal Society of London. Series A, Mathematical and Physical Sciences* 285(1327), pages 227–234. DOI: 10.1098/rsta.1977.0059.

Hunt, J. A., D. M. Pyle, and T. A. Mather (2019). "The Geomorphology, Structure, and Lava Flow Dynamics of Peralkaline Rift Volcanoes From High-Resolution Digital Elevation Models". *Geochemistry, Geophysics, Geosystems* 20(3), pages 1508–1538. DOI: 10.1029/2018gc008085.

Inomata, T., D. Triadan, V. A. Vázquez López, J. C. Fernandez-Diaz, T. Omori, M. B. Méndez Bauer, M. García Hernández, T. Beach, C. Cagnato, K. Aoyama, and H. Nasu (2020). "Monumental architecture at Aguada Fénix and the rise of Maya civilization". *Nature* 582(7813), pages 530–533. DOI: 10.1038/s41586-020-2343-4.

Israde-Alcántara, I., V. H. Garduño-Monroy, C. T. Fisher, H. P. Pollard, and M. A. Rodríguez-Pascua (2005). "Lake level change, climate, and the impact of natural events: the role of seismic and volcanic events in the formation of the Lake Patzcuaro Basin, Michoacan, Mexico". *Quaternary International* 135(1), pages 35–46. DOI: 10.1016/j.quaint.2004.10.022.

Jeffreys, H. (1925). "LXXXIV. The flow of water in an inclined channel of rectangular section". *The London, Edinburgh, and Dublin Philosophical Magazine and Journal of Science* 49(293), pages 793–807. DOI: 10.1080/14786442508634662.

Kereszturi, G. and K. Nmeth (2012). "Monogenetic Basaltic Volcanoes: Genetic Classification, Growth, Geomorphology and Degradation". *Updates in Volcanology - New Advances in Understanding Volcanic Systems*. InTech. ISBN: 9789535109150. DOI: 10.5772/51387.

Kilburn, C. R. J. (2015). "Lava Flow Hazards and Modeling". *The Encyclopedia of Volcanoes*. Elsevier, pages 957–969. ISBN: 9780123859389. DOI: 10.1016/b978-0-12-385938-9.00055-9.

Kilburn, C. R. J. and R. M. C. Lopes (1991). "General patterns of flow field growth: Aa and blocky lavas". *Journal of Geophysical Research: Solid Earth* 96(B12), pages 19721–19732. DOI: 10.1029/91jb01924.

Kshirsagar, P., C. Siebe, M.-N. Guilbaud, and S. Salinas (2016). "Geological and environmental controls on the change of eruptive style (phreatomagmatic to Strombolian-effusive) of Late Pleistocene El Caracol tuff cone and its comparison with adjacent volcanoes around the Zacapu basin (Michoacán, México)". *Journal of Volcanology and Geothermal Research* 318, pages 114–133. DOI: 10.1016/j.jvolgeores.2016.03.015.

Kshirsagar, P., C. Siebe, M.-N. Guilbaud, S. Salinas, and P. W. Layer (2015). "Late Pleistocene Alberca de Guadalupe maar volcano (Zacapu basin, Michoacán): Stratigraphy, tectonic setting, and paleo-hydrogeological environment". *Journal of Volcanology and Geothermal Research* 304, pages 214–236. DOI: 10.1016/j.jvolgeores.2015.09.003.

Kubanek, J., J. A. Richardson, S. J. Charbonnier, and L. J. Connor (2015). "Lava flow mapping and volume calculations for the 2012–2013 Tolbachik, Kamchatka, fissure eruption using bistatic TanDEM-X InSAR". *Bulletin of Volcanology* 77(12). DOI: 10.1007/s00445-015-0989-9.

Larrea, P., S. Salinas, E. Widom, C. Siebe, and R. J. Abbitt (2017). "Compositional and volumetric development of a monogenetic lava flow field: The historical case of Paricutin (Michoacán, Mexico)". *Journal of Volcanology and Geothermal Research* 348, pages 36–48. DOI: 10.1016/j.jvolgeores.2017.10.016.

Larrea, P., C. Siebe, E. Juárez-Arriaga, S. Salinas, H. Ibarra, and H. Böhnel (2019a). "The AD 500–700 (Late Classic) El Astillero and El Pedregal volcanoes (Michoacán, Mexico): a new monogenetic cluster in the making?" *Bulletin of Volcanology* 81(8), page 59. DOI: 10.1007/s00445-019-1318-5.

Larrea, P., E. Widom, C. Siebe, S. Salinas, and D. Kuentz (2019b). "A re-interpretation of the petrogenesis of Paricutin volcano: Distinguishing crustal contamination from mantle heterogeneity". *Chemical Geology* 504, pages 66–82. DOI: 10.1016/j.chemgeo.2018.10.026.

Larrea, P., E. Widom, C. Siebe, S. Salinas, and D. Kuentz (2023). "Deciphering the sources and processes feeding young monogenetic volcanoes from the Michoacán Guanajuato Volcanic Field (Mexico): A study case of El Astillero and El Pedregal". *Lithos* 456–457, page 107302. DOI: 10.1016/j.lithos.2023.107302.

LeBas, M., R. Maitre, A. Streckeisen, and B. Zanettin (1986). "A Chemical Classification of Volcanic Rocks Based on the Total Alkali-Silica Diagram". *Journal of Petrology* 27(3), pages 745–750. DOI: 10.1093/petrology/27.3.745.

Lefler, E. (2011). "Genauigkeitsbetrachtung bei der Ermittlung rheologischer Parameter von Lavaströmen aus Fernerkundungsdaten". Bachelor thesis. Freie Universität Berlin.

Legrand, D., M. Perton, J. L. Macías, C. Siebe, J. Pacheco, F. Chacón, J. Lermo, L. Quintanar, and G. Cisneros (2023). "Repeated seismic swarms near Paricutin volcano: precursors to the birth of a new monogenetic volcano in the Michoacán-Guanajuato volcanic field, México?" *Bulletin of Volcanology* 85(5). DOI: 10.1007/s00445-023-01645-0.

Lev, E., M. Spiegelman, R. J. Wysocki, and J. A. Karson (2012). "Investigating lava flow rheology using video analysis and numerical flow models". *Journal of Volcanology and Geothermal Research* 247–248, pages 62–73. DOI: 10.1016/j.jvolgeores.2012.08.002.

Luhr, J. F. and I. S. E. Carmichael (1985). "Jorullo Volcano, Michoacán, Mexico (1759–1774): The earliest stages of fractionation in calc-alkaline magmas". *Contributions to Mineralogy and Petrology* 90(2–3), pages 142–161. DOI: 10.1007/bf00378256.

Luhr, J. F. and T. Simkin (1993). *Paricutin: The volcano born in a Mexican cornfield*. U.S. Geoscience Press.

Mahgoub, A., N. Reyes-Guzmán, H. Böhnel, C. Siebe, G. Pereira, and A. Dorison (2018). "Paleomagnetic constraints on the ages of the Holocene Malpaís de Zacapu lava flow eruptions, Michoacán (México): Implications for archeology and volcanic hazards". *The Holocene* 28(2), pages 229–245. DOI: 10.1177/0959683617721323.

McAnany, P. A. (2020). "Large-scale early Maya sites in Mexico revealed by lidar mapping technology". *Nature* 582(7813), pages 490–492. DOI: 10.1038/d41586-020-01570-8.

Meredith, E. S., S. F. Jenkins, J. L. Hayes, N. I. Deligne, D. Lallemant, M. Patrick, and C. Neal (2022). "Damage assessment for the 2018 lower East Rift Zone lava flows of Kīlauea volcano, Hawai'i". *Bulletin of Volcanology* 84(7). DOI: 10.1007/s00445-022-01568-2.

Naranjo, J. A., R. S. J. Sparks, M. V. Stasiuk, H. Moreno, and G. J. Ablay (1992). "Morphological, structural and textural variations in the 1988–1990 andesite lava of Lonquimay Volcano, Chile". *Geological Magazine* 129(6), pages 657–678. DOI: 10.1017/s0016756800008426.

Navarro-Ochoa, C., J. Gavilanes-Ruíz, and A. Cortés-Cortés (2002). "Movement and emplacement of lava flows at Volcán de Colima, México: November 1998–February 1999". *Journal of Volcanology and Geothermal Research* 117(1-2), pages 155–167. DOI: 10.1016/S0377-0273(02)00242-1.

Nixon, G. T. (1982). "The relationship between Quaternary volcanism in central Mexico and the seismicity and structure of subducted ocean lithosphere". *Geological Society of America Bulletin* 93(6), page 514. DOI: 10.1130/0016-7606(1982)93<514:trbqvi>2.0.co;2.

Osorio-Ocampo, S., J. L. Macías, A. Pola, S. Cardona-Melchor, G. Sosa-Ceballos, V. H. Garduño-Monroy, P. W. Layer, L. García-Sánchez, M. Perton, and J. Benowitz (2018). "The eruptive history of the Pátzcuaro Lake area in the Michoacán Guanajuato Volcanic Field, central México: Field mapping, C-14 and 40Ar/39Ar geochronology". *Journal of Volcanology and Geothermal Research* 358, pages 307–328. DOI: 10.1016/j.jvolgeores.2018.06.003.

Ownby, S., H. Delgado Granados, R. A. Lange, and C. M. Hall (2007). "Volcán Tancítaro, Michoacán, Mexico, 40Ar/39Ar constraints on its history of sector collapse". *Journal of Volcanology and Geothermal Research* 161(1–2), pages 1–14. DOI: 10.1016/j.jvolgeores.2006.10.009.

Pardo, M. and G. Suárez (1995). "Shape of the subducted Rivera and Cocos plates in southern Mexico: Seismic and tectonic implications". *Journal of Geophysical Research: Solid Earth* 100(B7), pages 12357–12373. DOI: 10.1029/95jb00919.

Pereira, G., M. Forest, E. Jadot, and V. Darras (2021). "Ephemeral cities? The longevity of the Postclassic Tarascan urban sites of Zacapu Malpaís and its consequences on the migration process". *Mobility and Migration in Ancient Mesoamerican Cities*. Edited by A. M.-C., B. C., and G. Pereira. University Press of Colorado, Louisville, pages 208–231.

Pérez-Orozco, J., G. Sosa-Ceballos, V. Garduño-Monroy, and D. Avellán (2018). "Felsic-intermediate magmatism and brittle deformation in Sierra del Tzirate (Michoacán-Guanajuato Volcanic Field)". *Journal of South American Earth Sciences* 85, pages 81–96. DOI: 10.1016/j.jsames.2018.04.021.

Pinkerton, H. and R. Sparks (1976). "The 1975 sub-terminal lavas, mount etna: a case history of the formation of a compound lava field". *Journal of Volcanology and Geothermal Research* 1(2), pages 167–182. DOI: 10.1016/0377-0273(76)90005-6.

Pistone, M., B. Cordonnier, P. Ulmer, and L. Caricchi (2016). "Rheological flow laws for multiphase magmas: An empirical approach". *Journal of Volcanology and Geothermal Research* 321, pages 158–170. DOI: 10.1016/j.jvolgeores.2016.04.029.

Pollard, H. P. (2008). "A model of the emergence of the Tarascan State". *Ancient Mesoamerica* 19(2), pages 217–230. DOI: 10.1017/s0956536108000369.

Pollard, H. P. and L. Cahue (1999). "Mortuary Patterns of Regional Elites in the Lake Patzcuaro Basin of Western Mexico". *Latin American Antiquity* 10(3), pages 259–280. DOI: 10.2307/972030.

Pollard, H. P., W. T. Sanders, A. G. Mastache, and R. H. Cobean (2003). "Central places and cities in the core of the Tarascan state". *Urbanism in Mesoamerica*, pages 345–390.

Putirka, K. D. (2008). "Thermometers and Barometers for Volcanic Systems". *Reviews in Mineralogy and Geochemistry* 69(1), pages 61–120. DOI: 10.2138/rmg.2008.69.3.

Ramírez-Uribe, I., C. Siebe, M. O. Chevrel, D. Ferres, and S. Salinas (2022). "The late Holocene Nealtican lava-flow field, Popocatépetl volcano, central Mexico: Emplacement dynamics and future hazards". *GSA Bulletin* 134(11–12), pages 2745–2766. DOI: 10.1130/b36173.1.

Ramírez-Uribe, I., C. Siebe, M. O. Chevrel, and C. T. Fisher (2021). "Rancho Seco monogenetic volcano (Michoacán, Mexico): Petrogenesis and lava flow emplacement based on LiDAR images". *Journal of Volcanology and Geothermal Research* 411, page 107169. DOI: 10.1016/j.jvolgeores.2020.107169.

Ramírez-Uribe, I., C. Siebe, S. Salinas, M.-N. Guilbaud, P. Layer, and J. Benowitz (2019). "14C and 40Ar/39Ar radiometric dating and geologic setting of young lavas of Rancho Seco and Mazcuta volcanoes hosting archaeological sites at the margins of the Pátzcuaro and Zacapu lake basins (central Michoacán, Mexico)". *Journal of Volcanology and Geothermal Research* 388, page 106674. DOI: 10.1016/j.jvolgeores.2019.106674.

Reyes-Guzmán, N., C. Siebe, M. O. Chevrel, M.-N. Guilbaud, S. Salinas, and P. Layer (2018). "Geology and radiometric dating of Quaternary monogenetic volcanism in the western Zacapu lacustrine basin (Michoacán, México): implications for archeology and future hazard evaluations". *Bulletin of Volcanology* 80(2). DOI: 10.1007/s00445-018-1193-5.

Reyes-Guzmán, N., C. Siebe, M. O. Chevrel, and G. Pereira (2021). "Late Holocene Malpaís de Zacapu (Michoacán, Mexico) andesitic lava flows: rheology and eruption properties based on LiDAR image". *Bulletin of Volcanology* 83(4). DOI: 10.1007/s00445-021-01449-0.

Reyes-Guzmán, N., C. Siebe, M. O. Chevrel, G. Pereira, A. N. Mahgoub, and H. Böhnel (2023). "Holocene volcanic eruptions of the Malpaís de Zacapu and its pre-Hispanic settlement history". *Ancient Mesoamerica* 34(3), pages 712–727. DOI: 10.1017/s095653612100050x.

Rowland, S., Z. Jurado-Chichay, G. Ernst, and G. Walker (2009). "Pyroclastic deposits and lava flows from the 1759–1774 eruption of El Jorullo, México: aspects of 'violent Strombolian' activity and comparison with Parícutin". *Studies in Volcanology: The Legacy of George Walker*. Edited by T. Thordarson, S. Self, G. Larsen, S. Rowland, and Á. Höskuldsson. Geological Society of London. ISBN: 9781862392809. DOI: 10.1144/IAVCEl002.6.

Sato, H., K. Suzuki-Kamata, E. Sato, K. Sano, K. Wada, and R. Imura (2013). "Viscosity of andesitic lava and its implications for possible drain-back processes in the 2011 eruption of the Shinmoedake volcano, Japan". *Earth, Planets and Space* 65(6), pages 623–631. DOI: 10.5047/eps.2013.05.018.

Siebe, C. (2000). "Age and archaeological implications of Xitle volcano, southwestern Basin of Mexico-City". *Journal of Volcanology and Geothermal Research* 104(1-4), pages 45–64. DOI: 10.1016/S0377-0273(00)00199-2.

Siebe, C., M.-N. Guilbaud, S. Salinas, P. Kshirsagar, M. O. Chevrel, J. De la Fuente, A. Hernández-Jiménez, and L. Godínez (2014). "Monogenetic volcanism of the Michoacán-Guanajuato Volcanic Field: Maar craters of the Zacapu basin and domes, shields, and scoria cones of the Tarascan highlands (Paracho-Paricutin region)". *Field Guide, Pre-Meeting Fieldtrip for the 5th International Maar Conference (5IMC-IAVCEI)*. Querétaro, pages 13–17.

Siebe, C., G. Pereira, A. Dorison, N. Reyes-Guzmán, I. Ramírez-Uribe, and O. Quezada-Ramírez (2023). "Archaeology and recent volcanism in the Zacapu lacustrine basin (Michoacán, Mexico): A guidebook for the post-meeting fieldtrip (February 24-26) in conjunction with the conference". *Celebrating the 80th Anniversary of Parícutin Volcano, Preserving our Heritage and Preparing for Future Eruptions*. Morelia, Mexico, page 44.

Siebe, C., V. Rodríguez-Lara, P. Schaaf, and M. Abrams (2004). "Geochemistry, Sr–Nd isotope composition, and tectonic setting of Holocene Pelado, Guespalapa and Chichinautzin scoria cones, south of Mexico City". *Journal of Volcanology and Geothermal Research* 130(1-2), pages 197–226. DOI: 10.1016/S0377-0273(03)00289-0.

Tsang, S. W. R. and J. M. Lindsay (2020). "Lava flow crises in inhabited areas part I: lessons learned and research gaps related to effusive, basaltic eruptions". *Journal of Applied Volcanology* 9(1). DOI: 10.1186/s13617-020-00096-y.

Tsang, S. W. R., J. M. Lindsay, G. Coco, R. Wysocki, G. A. Lerner, E. Rader, G. M. Turner, and B. Kennedy (2019). "The heating of substrates beneath basaltic lava flows". *Bulletin of Volcanology* 81(11). DOI: 10.1007/s00445-019-1320-y.

Valentine, G. A. and C. B. Connor (2015). "Basaltic Volcanic Fields". *The Encyclopedia of Volcanoes*. Elsevier, pages 423–439. ISBN: 9780123859389. DOI: 10.1016/b978-0-12-385938-9.00023-7.

Verolino, A., S. F. Jenkins, K. Sieh, J. S. Herrin, D. Schonwalder-Angel, V. Sihavong, and J. H. Oh (2022). "Assessing volcanic hazard and exposure to lava flows at remote volcanic fields: a case study from the Bolaven Volcanic Field, Laos". *Journal of Applied Volcanology* 11(1). DOI: 10.1186/s13617-022-00116-z.

Waters, L. E. and R. A. Lange (2015). "An updated calibration of the plagioclase-liquid hygrometer-thermometer applicable to basalts through rhyolites". *American Mineralogist* 100(10), pages 2172–2184. DOI: 10.2138/am-2015-5232.

Wieser, P., M. Petrelli, J. Lubbers, E. Wieser, S. Ozaydin, A. Kent, and C. Till (2022). "Thermobar: An open-source Python3 tool for thermobarometry and hygrometry". *Volcanica* 5(2), pages 349–384. DOI: 10.30909/vol.05.02.349384.

Wilcox, R. (1954). *Petrology of Parícutin Volcano Mexico*. U.S. Government Printing Office.

Younger, Z. P., G. A. Valentine, and T. K. P. Gregg (2019). "'A'ā lava emplacement and the significance of rafted pyroclastic material: Marcath volcano (Nevada, USA)". *Bulletin of Volcanology* 81(9). DOI: 10.1007/s00445-019-1309-6.